Thesis Report

On

Performance Evaluation of Vertical Cavity Surface Emitting and Distributed Feedback Lasers

Submitted in the partial fulfilment of requirement for the award of the degree of

MASTER OF ENGINEERING

IN

ELECTRONICS AND COMMUNICATION ENGINEERING

Submitted by

SURJEET SINGH

Roll No. 800861016

Under the guidance of

Dr. R.S. KALER
Professor, ECED
Thapar University, Patiala

Electronics and Communication Engineering Department

THAPAR UNIVERSITY

PATIALA-147004

July, 2010

Certificate

I hereby certify that the work which is being presented in the thesis entitled, "**Performance Evaluation of Vertical Cavity Surface Emitting and Distributed Feedback Lasers,**" in partial fulfilment of the requirements for the award of degree of Master of Engineering in Electronics and Communications engineering submitted in Electronics and Communication Engineering Department of Thapar University, Patiala, is an authentic record of my own work carried under the supervision of Dr. R.S. Kaler. The matter presented in this thesis has not been submitted for the award of any other degree of this or any other university.

Surjeet Singh

This is to certify that the above statement made by the candidate is correct and true to the best of my knowledge.

Dr. R.S. Kaler
Professor, ECED
Thapar University, Patiala

Dr. A.K. Chatterjee
Head, ECED
Thapar University, Patiala

Dr. R.K. Sharma
Dean, Academic Affairs
Thapar University, Patiala

ACKNOWLEDGEMENT

It is with the deepest sense of gratitude that I am reciprocating the magnanimity, which my guide **Dr. R.S Kaler**, Professor, Electronics and Communication Engineering Department, has bestowed on me by providing individual guidance and support throughout the thesis work.

I am also thankful to **Dr. A. K. Chatterjee**, Head, Electronics and Communication Engineering Department and **Ms. Alpana Agarwal**, P.G. Coordinator, ECED for the motivation and inspiration that triggered me for my thesis work.

I would also like to thank all the staff members and my co-students who were always there at the need of the hour and provided with all the help and facilities, which I required for the completion of my thesis. I am also thankful to the authors whose works I have consulted and quoted in this work.

Last but not the least I would like to thank God for not letting me down at the time of crisis and showing me the silver lining in the dark clouds.

Surjeet Singh

Roll No. 800861016

Abstract

Optical fibers are not only used in the telecommunication but also used in the Internet and Local Area Networks (LAN) to achieve high signalling rates. Optical networks, based on the emergence of the optical layer in transport networks, provide higher capacity and reduced costs for new applications such as the Internet, video and multimedia interaction, and advanced digital services. The data rate through fiber largely depends upon the transmitter in which key component is laser which is used as optical source. The objective of the thesis work is to optimization of parameters for vertical cavity surface emitting laser (VCSEL) and Distributed Feedback Laser (DFB).

The effect of change in ambient temperature is studied for VCSEL with the help of output power evaluation. It is observed that output power decrease with increase in ambient temperature which degrades its performance at high temperature. If a laser is designed with lower threshold voltage the effect of decrease in power due to increase in ambient temperature can be compensated. Propagation of VCSEL signal from single mode and multimode fibers is studied. A VCSEL output signal directly modulated can travel 125 m through multimode fiber and up to 3.7km on single mode fiber.

Advantage of direct modulations is that it is easier to implement but it limits the data rate. For higher data rates data should be directly modulated. By using DFB laser which is drived at different values of driving current. Light current characteristics shows that output power increase with increase in driving current up to certain value and after that it gets saturated. But bit error rate first decrease and after certain value it again starts increasing. Driving current is optimized for minimum bit error rate. Comparison between various modulation coding formats combined with modulation techniques is made at the optimized value of the driving current. The coding formats analysed are NRZ: Rectangular, NRZ: Raised cosine, RZ: Rectangular and RZ: Raised cosine. Modulation techniques used are amplitude and phase modulation. After analysing the simulation results it is observed that NRZ rectangular coding format combined with phase modulator give best results with acceptable BER up to longer distance.

Table of Contents

Certificate.....iv

Acknowledgement.....iv

Abstract.....iv

Table of Contents.....iv

List of Figures.....iv

List of Abbreviations.....iv

List of Symbols..... iv

Chapter 1: Introduction.....1-20

1.1 Importance of Optical Communication.....1

1.2 LASER.....2

1.2.1 LASER Principle.....3

1.2.2 Basic Semiconductor Laser Design.....5

1.2.3 Vertical Cavity Surface Emitting Laser (VCSEL).....6

1.2.4 Distributed Feedback Laser.....10

1.3 Optical Fiber.....13

1.3.1 Single Mode Fiber Vs Multimode Fiber.....14

1.4 Introduction to OptSim.....15

1.4.1 System Requirements.....16

1.4.2 Simulation.....16

1.4.3 Analysis.....16

1.5 Modulation Formats.....17

1.5.1 Non-return-to-zero (NRZ) Modulation format.....18

1.5.2 Return-to-zero (RZ) modulation format 18

1.6 Thesis Objective.....19

1.7 Thesis Organization.....20

Chapter-2 Literature Review.....21-25

Chapter-3 Performance evaluation of VCSEL at various physical parameters and propagation through single and multi mode fibers.....26-34

3.1 Abstract.....26

3.2 Introduction.....26

3.3 Simulation Setup..... .27

3.4 Result and discussions 29

3.5 Conclusion.....34

Chapter 4 Performance evaluation of DFB laser using different modulation techniques and coding formats with the optimization of bias current.....35-45

4.1 Abstract.....35

4.2 Introduction.....35

4.3 Simulation Setup.....37

4.4 Result and Discussions.....38

4.5 Conclusion.....45

Chapter 5 Conclusion and Future Work.....46-47

5.1 Conclusions.....46

5.2 Future Work.....47

References.....48-52

List of Figures

Figure No.	Figure Name	Page No
Figure 1.1	Typical Optical Cavity of a Laser	3
Figure 1.2	Energy State Diagram showing: (a) spontaneous recombination (photon emission); (b) stimulated generation (photon absorption); (c) stimulated recombination (coherent photon emission); (d) nonradiative recombination	4
Figure 1.3	A generic p-n junction laser	5
Figure 1.4	The oxide-confined VCSEL emitting through the top DBR	8
Figure 1.5	Three periods of a distributed Bragg reflector	9
Figure 1.6	Optical gain as function of the emission wavelength with the MQW temperature Ta as parameter	9
Figure 1.7	I-L Characteristics with temperature as parameter	10
Figure 1.8	DFB Laser Structure	11
Figure 1.9	Field penetration into a Bragg mirror	12
Figure 1.10	The low-attenuation regions of an optical fiber	13
Figure 1.11(a)	Single-Mode Optical fiber	14
Figure 1.11(b)	Multimode Optical Fiber	15
Figure 1.12	The OptSim graphical editor	17
Figure 1.13	Optical spectrum of NRZ modulation format	18
Figure 1.14	Optical spectrum of RZ modulation format	19
Figure 3.1(a)	Setup for analysing the effect of temperature	28
Figure 3.1(b)	Setup for Propagation through SM and MM fiber	29
Figure 3.2	Temperature Vs Output Power	29
Figure 3.3	Threshold voltage Vs Output Power	20
Figure 3.4	Distance Vs BER	30

Figure 3.5	Distance Vs Q factor	31
Figure 3.6	Eye Diagram for MM fiber at 125m With BER 10^{-9}	31
Figure 3.7	Eye diagram for SM fiber at 3.7 km with BER 10^{-9}	32
Figure 3.8	Output signal for MM fiber at 125 meter	32
Figure 3.9	Output signal for SM fiber at 3.7 km	33
Figure 3.10	Distance Vs Eye opening	33
Figure 4.1(a)	Simulation Setup for optimization of bias current	37
Figure 4.1(b)	Simulation Setup for optimization of modulation formats	38
Figure 4.2	Bias current Vs Output Power	38
Figure 4.3	Bias Current Vs Bit Error Rate	39
Figure 4.4	Bias Current Vs Q Factor	39
Figure 4.5	Optical Spectrum at I_{bias}=30 mA	40
Figure 4.6	Optical Spectrum at I_{bias}=40 mA	40
Figure 4.7	Optical Spectrum at I_{bias}=50 mA	41
Figure 4.8	Eye Diagram at $I_{bias=}$30 mA	41
Figure 4.9	Eye Diagram at $I_{bias=}$40 mA	42
Figure 4.10	Eye Diagram at I_{bias} =50 mA	42
Figure 4.11	Distance Vs BER using Amplitude Modulation at I_{bias}=40 mA	43
Figure 4.12	Distance Vs BER using Phase Modulation at I_{bias}=40 mA	43
Figure 4.13	Distance Vs Eye Opening using Amplitude Modulation	44
Figure 4.14	Distance Vs Eye opening using Phase modulation	44

LIST OF ABBREVIATIONS

BER	Bit error rate
DBR	Distributed brag reflectors
DFB	Distributed feed back
EDFA	Erbium doped fiber amplifier
E_c	Energy of conduction band
E_v	Energy of valance band
FP	Fabry parot
MM	Multi mode fiber
MQW	Multi quantum well
RZ	Return to zero
NRZ	Non return to zero
SM	Single mode fiber
VCSEL	Vertical cavity surface emitting laser
WDM	Wavelength division multiplexing
RIN	Relative intensity of noise

List of Symbols

λ	Wavelength of light
c	Velocity of light
μm	Micro meter
nm	Nano meter
Km	Kilo meter
dB	Decibel
mA	Mili ampere
mW	Mili watt
Gb/s	Giga bit per second
ps	Pico second
°C	Degree Celsius
A	Ampere
V	Volt

Chapter 1: Introduction

1.1 Importance of Optical Communication

Twenty first century is the era of 'Information technology'. There is no doubt that information technology has an exponential growth through the modern telecommunication systems. Particularly, optical fiber communication plays a vital role in the development of high quality and high-speed telecommunication systems. Fiber optic communication is a way of exchanging the information between two places by sending the light signal through the optical fiber cable. Fiber optic communication brought the revolutionary change in the telecommunication industry and played a major role in the advent of information age. In the twenty first century, its advantages over electrical transmission cause the replacement of copper wire with the optical fiber in the communication system. Now the optical fiber is the most common type of channel used in communication system, but the other types of waveguides are also used within the communication system. Today, optical fibers are not only used in telecommunication links but also used in the Internet and local area networks (LAN) to achieve high signalling rates. The core advantages of optical fiber such as low loss, which allows long distances between amplifiers and its high data carrying capacity as that of thousands of electrical links would be required to carry that much data. Also no cross talk introduces in optical fibers running alongside each other for long distances as introduces in some types of electrical transmission lines. The use and demand for optical fiber has grown tremendously and optical-fiber applications are numerous. Telecommunication applications are widespread, ranging from global networks to desktop computers. These involve the transmission of voice, data, or video over distances of less than a meter to hundreds of kilometers, using one of a few standard fiber designs in one of several cable designs [1].

The role of optical transmitter is to convert an electrical input signal into the corresponding optical signal and then launch it into the optical fiber serving as the transmission medium. LED's are typically used in multimode transmission systems where data rates no larger than 50 Mb/s are required. They have larger spectral widths and can add to the problem of dispersion in communications systems. Laser diodes are used in systems that require coherent and often single mode light such as high data rate communications and sensing applications. In comparison to laser diodes, LED's can generally be driven harder, are less expensive, have

lower power, have larger emitting regions, and longer lifetimes. Lasers, unlike LED's will not operate below a threshold current. Meaning, only when the threshold current is reached will the diode commence lasing (functioning). As mentioned previously, LEDs and laser diodes are temperature sensitive when considering overall lifetime, for example, operating a laser diode at 10 °C higher than rated will half the life of the diode. Also a laser usually will stop functioning at 100°C. The degradation modes that result in failures or gradual degradation of these devices can be modelled using Arrhenius relationships where each degradation mode carries specific activation energy. For example in reliability tests in which lifetime is based on temperature aging the relationship is life = A $e^{Ea/kT}$. With increase in temperature or with time lasers starts degrading. The main degradation modes are: dislocations that affect the inner region, metal diffusion and alloy reaction that affect the electrode, solder instability (reaction and migration) that affect the bonding parts, separation of metals in the heat sink bond, and defects in buried heterostructure devices. These modes are enhanced by current during ambient temperature operations. Facet damage due to oxidation is enhanced by light or moisture and is particular to laser diodes [2].

1.2 LASER

A laser is an electronic optical device that beams strong light radiations. What laser does is, it emits light rays in a very narrow, single colored beam with certain wavelength. It is quite different from say a light bulb which throws light over a very wide area at variable wavelengths. The optical light source can be in the form of wide-band "continuous spectra" sources (i.e. incandescent lamps), monochromatic incoherent sources (i.e. LEDs) and monochromatic coherent sources (i.e. Lasers). Its primary purpose is to convert electrical energy in the form of current into optical energy in an efficient manner which allows the light output to be effectively launched or coupled into the optical fiber. The term LASER stands for Light Amplification by Stimulated Emission of Radiation. The operation of the device can be described by the formation of an electromagnetic wave within an optical cavity created by two mirrors at both ends of the laser. The electromagnetic wave moves inside the cavity from right to left through internal reflections by the two mirrors. The mirrors serve to increase the length of the active medium, by making the beam pass through the cavity many times, and they determine the boundary conditions for the electromagnetic fields inside the laser cavity. The mirrors, axially arranged around an intervening volume, allow only certain frequencies of electromagnetic radiation to set up standing waves [3]. These allowed frequencies of

oscillation are referred to as longitudinal modes of the cavity and are determined by the length of the cavity and the index of refraction of the active medium. The axis connecting the centers of these mirrors and perpendicular to them is called the optical axis of the laser and the aperture is the element within a cavity that limits the size of the laser beam [3]. The amplitude of a light beam is also increased by multiple passes of coherent light waves through the active medium. This process is accomplished by an active medium placed between a pair of mirrors that act as a feedback mechanism. During each round trip of the cavity, the beam passes through the active medium twice and is amplified. Some of the light passes through the output coupler to form output beam while some of the light is lost from the beam due to internal losses in the cavity. The remaining portion of the light is reflected back into the optical cavity. Thus through these processes, a laser beam, which is in the form of a monochromatic highly coherent radiation is ejected out of the laser in the direction of the optical axis. Fig. 1.1 shows an illustration of a typical optical cavity of a laser [4].

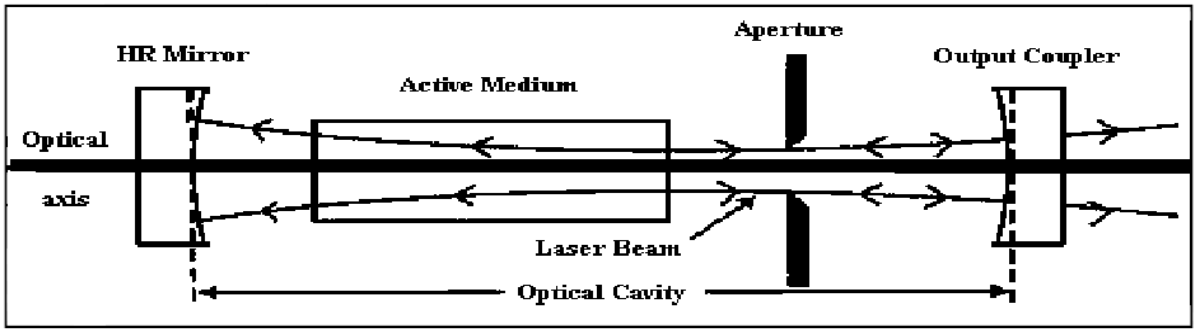

Fig 1.1 Typical Optical Cavity of a Laser [4]

1.2.1 LASER Principle

Lasing action is a process that occurs in matter. Since matter is composed of atoms, to gain an understanding of the light-generating mechanisms within a laser, it is necessary to consider the fundamental atomic concepts. From quantum theory, atoms exist only in certain discrete states such that the absorption and emission of light causes them to make a transition from one energy state to another. Figure 1.2 illustrates the different kinds of electronic transitions that are important [4].

Figure 1.2(a) represents the incident when an electron in the conduction band recombines spontaneously with a hole in the valence band to generate a photon. This process is the primary mechanism behind the light emitting diode (LED) as the photons generated would not contribute to a coherent radiation field due to random emission time and direction. The

second process in figure 1.2(b) occurs when a photon is absorbed and stimulates the generation of an electron in the conduction band while leaving a hole in the valence band.
The third process in figure 1.2(c) occurs when an incident photon stimulates the recombination of an electron and hole, and simultaneously generates a photon. The photon generated by stimulated emission is generally of an identical energy to the one that caused it and hence the light associated with them is of the same frequency, phase and polarization [5]. Stimulated emission thus produces coherent radiation that ultimately gives the laser its special properties as an optical source.

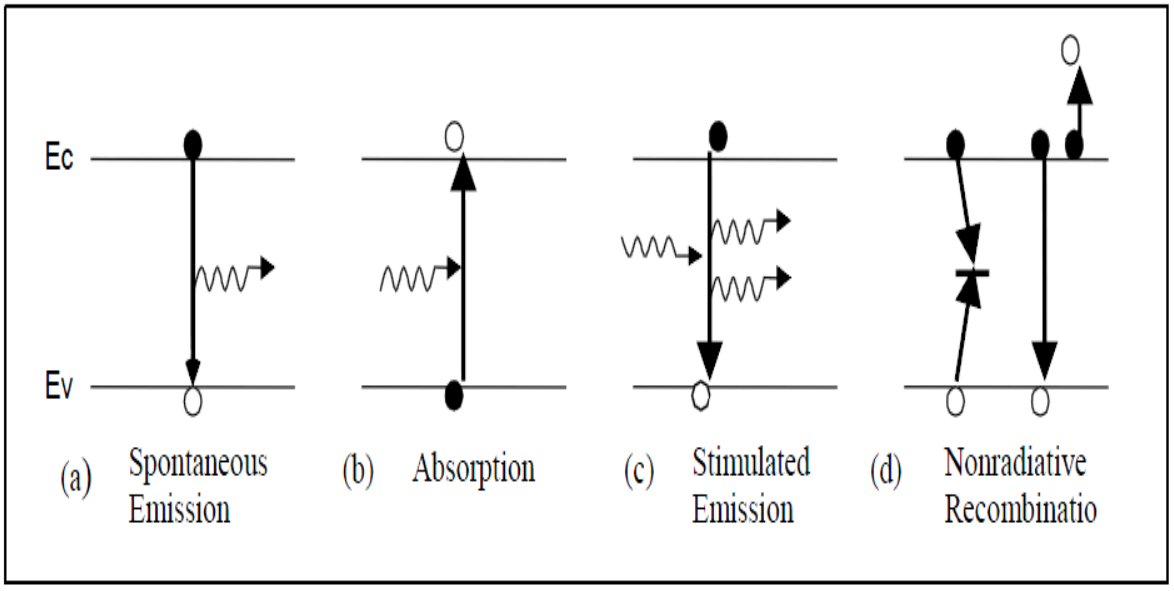

Figure 1.2 Energy State Diagram showing: (a) spontaneous recombination (photon emission); (b) stimulated generation (photon absorption); (c) stimulated recombination (coherent photon emission); (d) nonradiative recombination [5].

The open circle represents holes and the solid circles represent electrons. The final process in figure. 2.1(d) represents the several nonradiative ways in which a conduction band electron can recombine with a valence band hole without generating any useful photons. The energy is dissipated as heat in the semiconductor crystal lattice and these effects are undesirable. The two general nonradiative mechanisms illustrated are nonradiative recombination centers (point defects, surfaces and interfaces) in the active region and Auger Recombination. Auger recombination occurs when the electron-hole recombination energy is given to another electron or hole in the form of kinetic energy [4]. In order to achieve optical amplification, it is necessary to create a nonequilibrium distribution of atoms in the active medium such that

the population of the upper energy level is greater than the lower energy level. If a population inversion exists between two energy levels, the probability is high that an incoming photon will stimulate an excited atom to return to a lower state, while emitting another photon of light. The excitation mechanism (pumping) is the source of energy that raises the atoms in the active medium into their excited state, thus creating population inversion.

1.2.2 Basic Semiconductor Laser Design

Semiconductor lasers are diodes that emit coherent light by stimulated emission. They consist of a p-n junction inside a slab of semiconductor that is typically less than a millimeter in any dimension. Excitation is provided by current flow through the device, and the cleaved ends of the diode provide the feedback mirrors. Semiconductor lasers have important applications in communications and range finding. Basically, semiconductors are materials that have electrical conductivity intermediate between the high conductivity of metals and the low conductivity of insulators. The most common semiconductor material that has been used in lasers is gallium arsenide, GaAs. Fig. 1.3 shows the structure of the simplest (and earliest) type of gallium arsenide laser [4].

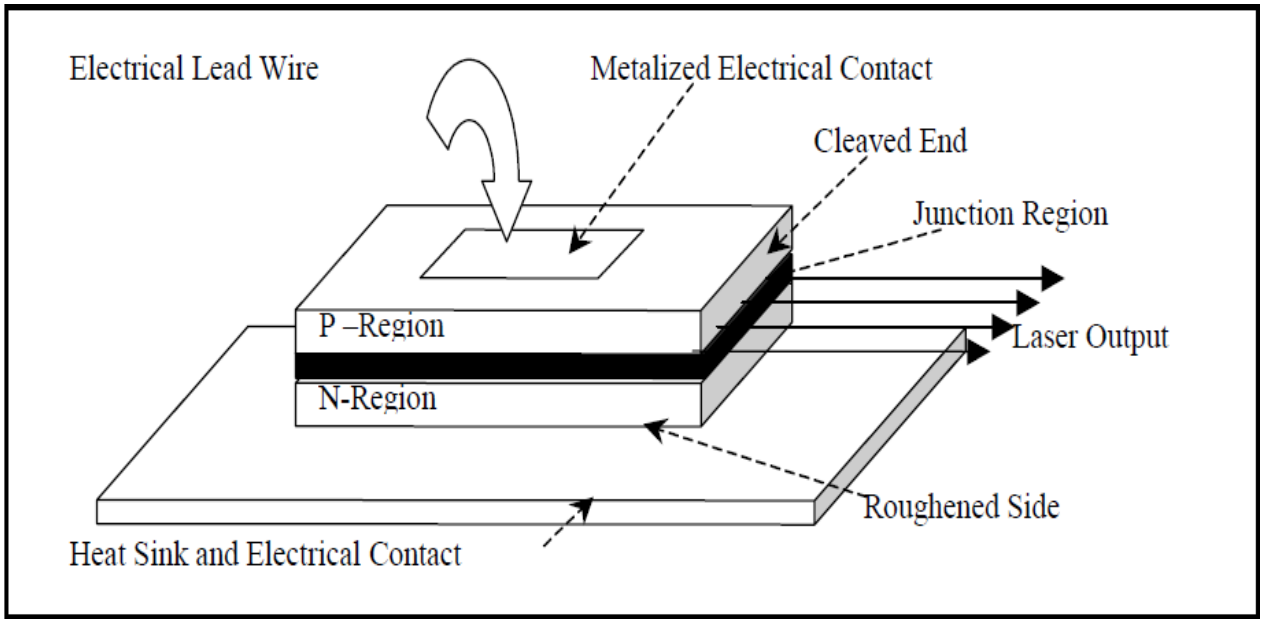

Figure. 1.3 A generic p-n junction laser [4].

In figure 1.3 the active region is at the junction of the p and n regions where the current is flowing. The cleaved ends of the laser act as partial mirrors in order to encourage stimulated emission in the cavity when electrons are injected into the p-type region. The reflectivity at

the interface between gallium arsenide and air is approximately 36% [6]. Excitation most often is provided by current flow (injection) through the active medium. The active region is the region where recombining carriers contribute to useful gain and photon emission. It is usually the lowest bandgap region within the depletion region of a pin diode for efficient injection.

The output power available from this laser is limited by the loop gain available within the laser cavity. The amplifier gain of the active medium is dependent on the current density through the junction. Higher currents produce greater power, but higher currents also increase heating effects that can damage the device [3].

However the device in Fig.1.3 has a high threshold current density due to the lack of carrier containment and proves to be an inefficient light source. Improved carrier containment and thus lower current densities can be achieved using heterojunction structures which basically are GaAs laser diodes with an advanced junction design to reduce diffraction loss in the optical cavity. This is accomplished by modification of the laser material to control the index of refraction of the cavity and the width of the junction [5].

1.2.3 Vertical Cavity Surface Emitting Laser (VCSEL)

Basically, the advantages that VCSELs have over in-plane lasers for short optical interconnects can be classified into two broad categories: cost and performance. Some of the advantages are:

- VCSELs are easier to test and package as device testing and burn-in can be done directly on wafer, thus allowing for automation for such processes. In-plane lasers on the other hand need to be cleaved into bars and tested individually, a labour-intensive process.
- Fiber coupling to VCSELs is more efficient due to its circular shape, vertically lasing action and small numerical aperture of the output beam; allowing for less expensive lens elements and increased alignment tolerances [7]. This advantage is not shared with in-plane lasers, which often require a lens element for high efficiency coupling to the fiber.
- The VCSEL's inherently smaller active region volumes and extremely high reflective mirrors, compared to in-plane lasers, allow the laser to achieve lower threshold currents. This is important as response speed is increased and turn-on delay decreased by operating the VCSEL with currents well above the threshold current. Thresholds

below 1 mA and high efficiency at the operating current also allows the laser to minimize the drive power requirements and minimize on-chip thermal dissipation, [8]. These requirements appear to be better met by VCSELs than in-plane lasers.

From the above points mentioned, it can be seen that especially for the area of high speed optical interconnects up to the LAN level, VCSELs show huge potential for commercial success. With applications for its use increasing dramatically, future products will exploit the multi-channel advantages of VCSEL arrays in parallel or WDM link modules.

The first vertical-cavity surface-emitting laser (VCSEL) was reported by Japanese scientists in 1979 [6]. Due to technical difficulties the VCSEL did not bloom until the early 1990s, where improvements in epitaxial growth technology made the growth of wafers for VCSEL fabrication cheaper and more reliable. Since then the VCSEL has evolved rapidly, and it has penetrated the short-range data-communication market. Future possible applications include laser line-of-sight data-communication, in which parallel data communication between e.g. two high buildings is performed using VCSEL arrays, optical interconnects, in which VCSELs are used for internal data transfer in computers, high-density optical storage, such as CD- and DVD burning, and laser printing, all of which require high output powers and good output beam characteristics [9].

Such lasers may be used for pumping of Erbium-doped fiber amplifiers (EDFAs) and may therefore be able to penetrate the telecommunication market. The technology behind such VCSELs is very well established; they are implemented using AlAs, GaAs, AlGaAs and InGaAs semiconductor materials, the technology of which is very mature [8]. In this section the oxide-confined VCSEL structure is introduced. The optical properties are described along with the merits and demerits of such VCSELs, and a brief summary is provided.

Several different VCSEL schemes exist, the most successful being the oxide confined VCSEL. This structure has demonstrated record low threshold current and wall-plug efficiencies, i.e. electrical-to-optical power conversion efficiencies, better than 55% [8].

A schematic of the oxide-confined VCSEL is shown in Figure 1.4 In this VCSEL scheme both electrical- and optical confinement is achieved by an oxide aperture near the active layer. The oxide, shown as a thin, black line above the optical cavity in the figure, is non-conductive and the current is therefore guided through the aperture in the center of the VCSEL. This effective current confinement allows for a high internal quantum efficiency, i.e. a large fraction of the current injected into the laser generates carriers in the active region. Also, the oxide has a much lower refractive index than the material in the center of the

aperture (n=1.6 vs. n=3.2), and the aperture therefore confines the optical field to the center of the VCSEL.

The top- and bottom mirrors in the oxide-confined VCSEL are distributed Bragg reflectors (DBRs), which provide very high reflectivities. The DBRs and the substrate, upon which the VCSEL is fabricated, are doped to allow for current transportation through the laser.

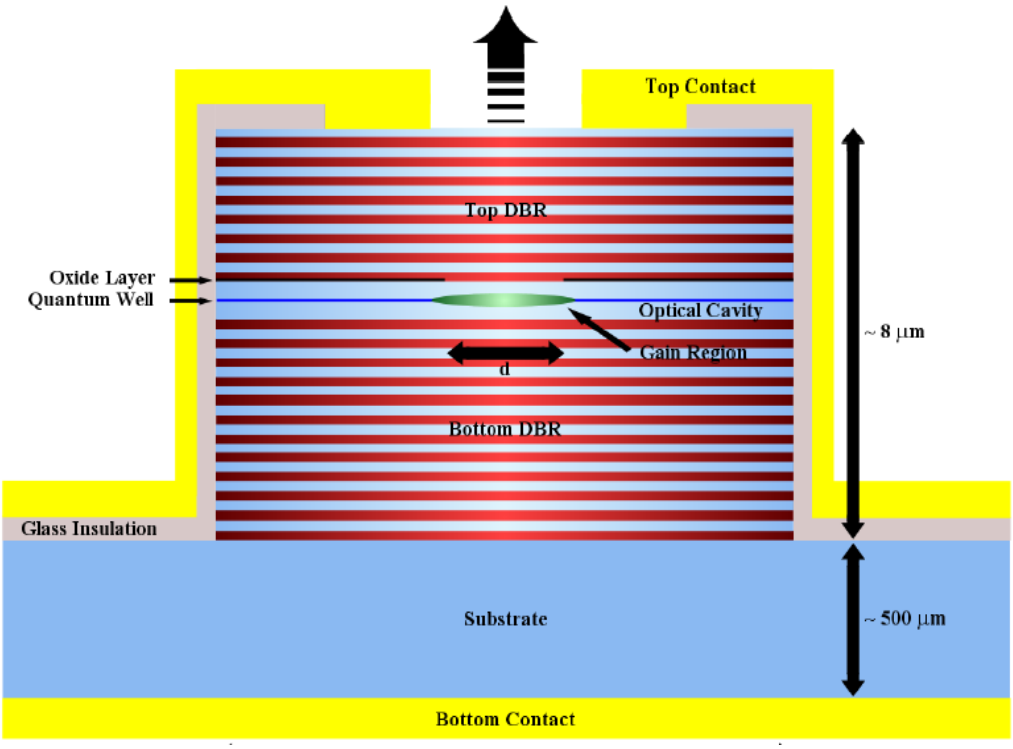

Figure 1.4: The oxide-confined VCSEL emitting through the top DBR.

The thin aperture layer, shown in black directly above the optical cavity, provides both electrical- and optical confinement, and thereby defines the diameter of the optical output beam.

Layers	Thickness	Material	Refractive Index
Top DBR (24.5 Periods)	69.49 nm 79.63 nm	GaAs AlGaAs	3.53 3.08
Aperture	15.93 nm	AlO_x	1.60
Cavity	136.49 nm 5.00 nm 136.49 nm	GaAs QW GaAs	3.53 3.53 3.53
Bottom DBR (29.5 periods)	79.63 nm 69.49 nm	AlGaAs GaAs	3.08 3.53

Table 1.1 Dimensions, material and refractive index of various layers for oxide confined VCSEL

To achieve such high reflectivity distributed Bragg reflectors (DBRs) are used. DBRs consist of many layers of alternating refractive index, so that at each interface there is a small reflection, as shown in Figure 1.5.

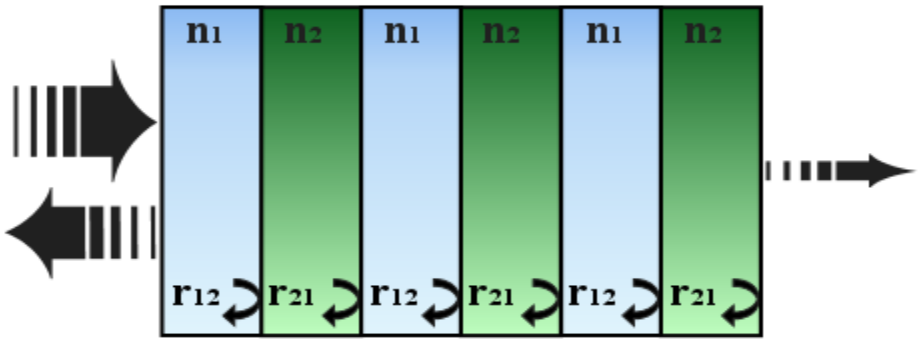

Figure 1.5 Three periods of a distributed Bragg reflector, with layers of alternating refractive index, providing small reflections at each layer interface.

VCSEL's have many advantages due to its small size and single longitudinal mode, Due to which it is easy to test on wafer. Due to increasing demand of data rates there are great improvements in basic characteristics of the laser which include output optical power. For reliable operation of the laser at high temperatures it is necessary to compensate the effects of the increase in temperature.

With rise in temperature there is shift in gain peak with respect to temperature. This results, decrease in output power of the laser. Fig 1.6 shows the effect of rise in temperature on the gain peak and output wavelength of the laser. Operating the laser at high temperatures this shift should be minimum otherwise it would affect the system. For reliable operation of the communication system, it should be less sensitive to temperature effects [10].

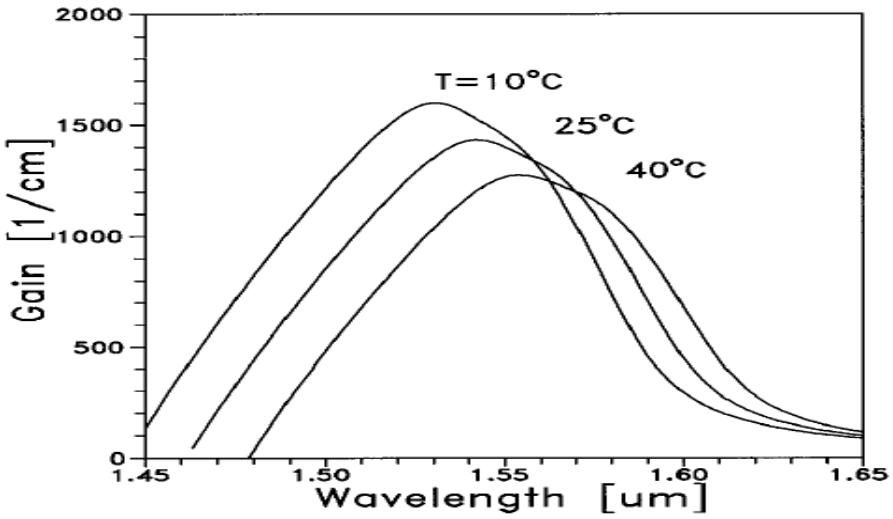

Fig 1.6 Optical gain as function of the emission wavelength with the MQW temperature as parameter [10]

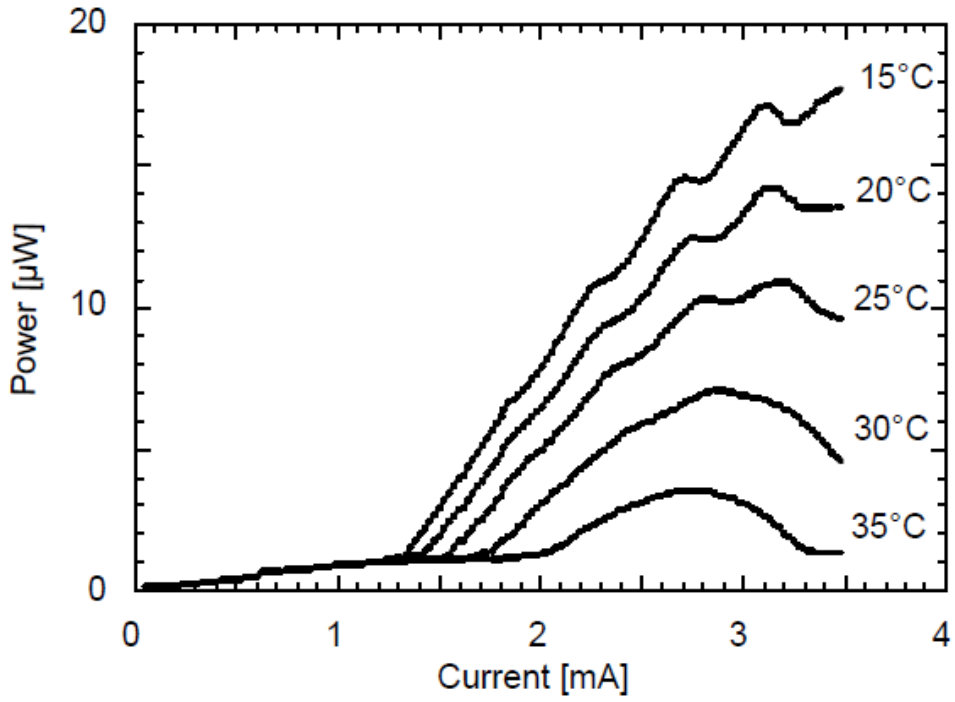

Fig. 1.7 I-L Characteristics with temperature as parameter [11]

Fig 1.7 shows variation of the output power with respect to driving current. If current is kept constant and temperature is varied there is significant decrease in the output power. This can be compensated by increasing the driving current. But increasing the driving current decrease the reliability and life of the laser. It is observed that with decrease in threshold voltage of laser its output power increase which is opposing the effect of rise in temperature. Laser design with lower threshold voltage will be suitable to operate it at high temperature with long life [11].

1.2.4 Distributed Feedback Laser

Distributed feedback (DFB) laser diodes are widely used as light sources in high-bit-rate and long-distance optical communication systems. It is an edge emitting device. Two types of DFB laser diodes are installed in the actual systems. One is a 1300 nm DFB laser diode whose wavelength corresponds to the zero dispersion region of an optical fiber [12]. The other is a 1550 nm DFB laser diode whose wavelength corresponds to the minimum loss region of an optical fiber [13]. In the 1980's, much effort was dedicated to realize low threshold and stable single-longitudinal-mode bulk DFB laser diodes [14]. In the early development stage, threshold currents were very large, for example, 250 mA for the 1.55 μm DFB laser diode and 66 mA for the 1300 m DFB laser diode. The internal loss of a cavity of a longer wavelength laser diode is larger than that of the shorter wavelength laser diode.

Therefore the threshold currents of the 1550 nm laser diode are expected to be larger than those of the 1300 nm laser diode [15].

The principle light oscillator used in optoelectronic applications will be the semiconductor laser, since it's extremely compact, simple, efficient, reliable, and economical nature is obviously advantageous. However, its relatively deficient spectral stability and purity prevent it from being widely accepted in the fields where highly coherent light is needed. The distributed feedback (DFB) structure, in which backward Bragg scattering resulting from such a periodic structure as built-in diffraction grating provides optical feedback, is one of the solutions for improving the spectral characteristics of semiconductor lasers. In the DFB laser, a longitudinal mode adjacent to the Bragg wavelength is selectively fed back, hence single longitudinal mode operation is allowed in spite of the broad gain spectrum of the semiconductors. The elimination of the mode hopping also gives low noise property and continuously-tunable capability to the laser. The fact that the laser does not require cleaved facet mirrors yields another significant feature, namely, compatibility with monolithic integration with other optical components. These particular advantages together with the other common merits of semiconductor lasers allow us to think of diverse applications [16]. Fig 1.8 shows a typical structure of DFB laser structure.

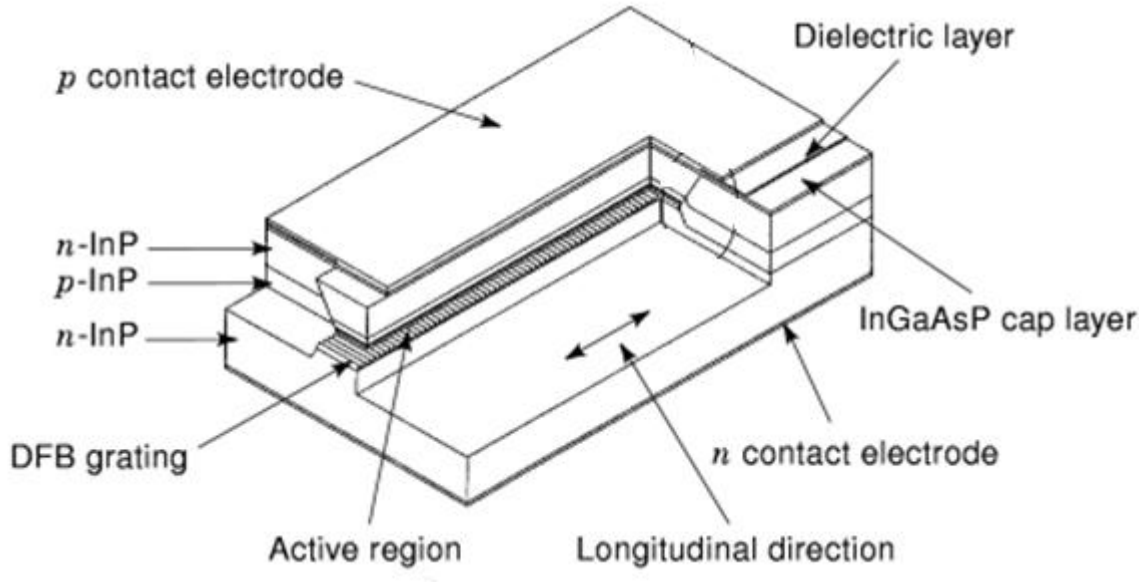

Fig 1.8 DFB Laser Structure [14]

It is a laser where the whole resonator consists of a periodic structure, which acts as a distributed reflector in the wavelength range of laser action, and contains a gain medium. Typically, the periodic structure is made with a phase shift in its middle. This structure is

essentially the direct concatenation of two Bragg gratings with internal optical gain. It has multiple axial resonator modes, but there is typically one mode which is favoured in terms of losses (This property is related to the above-mentioned phase shift.) Therefore, single-frequency operation is often easily achieved. A Bragg mirror (also called distributed Bragg reflector) is a structure which consists of an alternating sequence of layers of two different optical materials. The most frequently used design is that of a quarter-wave mirror, where each optical layer thickness corresponding to one quarter of the wavelength for which the mirror is designed. The latter condition holds for normal incidence; if the mirror is designed for larger angles of incidence, accordingly thicker layers are needed [15].

The principle of operation can be understood as follows. Each interface between the two materials contributes a Fresnel reflection. For the design wavelength, the optical path length difference between reflections from subsequent interfaces is half the wavelength; in addition, the reflection coefficients for the interfaces have alternating signs. Therefore, all reflected components from the interfaces interfere constructively, which results in a strong reflection. The reflectivity achieved is determined by the number of layer pairs and by the refractive index contrast between the layer materials. The reflection bandwidth is determined mainly by the index contrast. Figure 1.9 shows the field penetration into a Bragg mirror made of eight layer pairs of TiO_2 and SiO_2. The blue curve shows the intensity distribution of a wave with the design wavelength of 1000 nm, incident from the right-hand side. Note that the intensity is oscillating outside the mirror due to the interference of the counter propagating waves. The gray curve shows the intensity distribution for 800 nm, where a significant part of the light can get through the mirror coating [14].

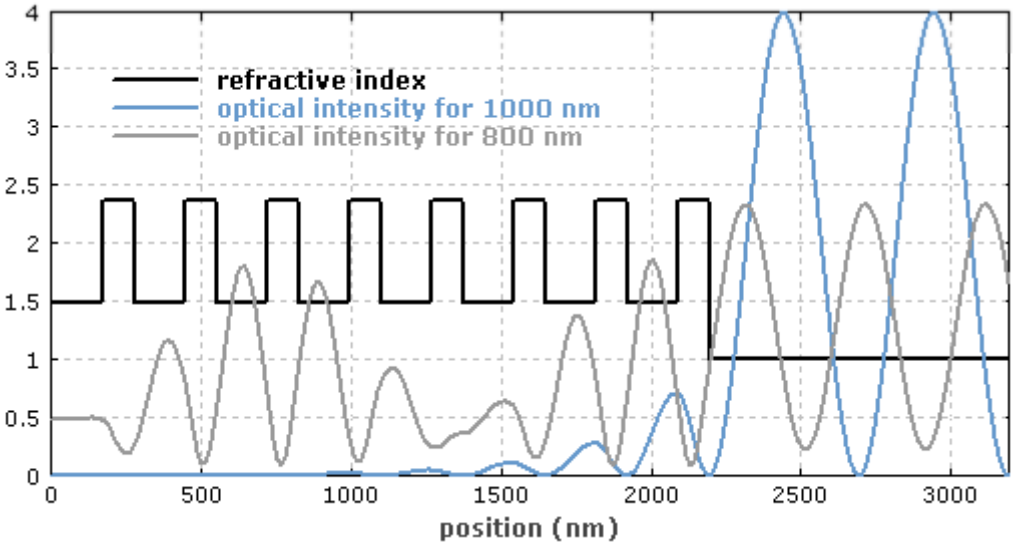

Fig 1.9 Field penetration into a Bragg mirror [14]

1.3 Optical Fiber

Fiber possesses many characteristics that make it an excellent physical medium for high-speed networking. Figure 1.10 shows the attenuation (and dispersion) characteristics of optical fiber.

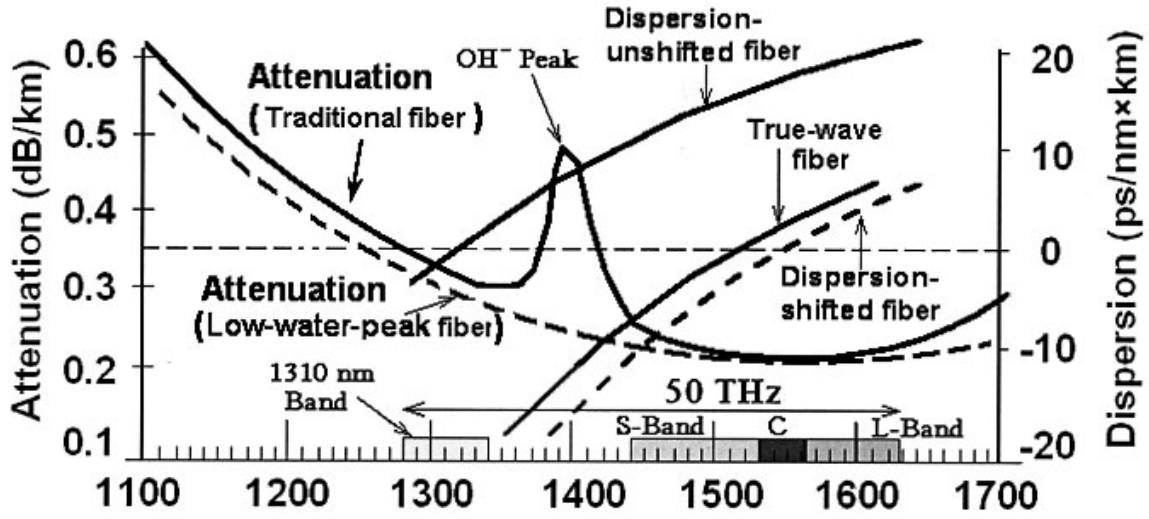

Fig 1.10 The low-attenuation regions of an optical fiber [28].

For traditional fiber, centered at approximately 1310 nm is a window of 200 nm in which attenuation is less than 0.5 dB/km. The total bandwidth in this region is about 25 THz. Centered at 1550 nm is a window of similar size, with attenuation as low as 0.2 dB/km, which consists of three bands, i.e., S-band (1460-1530 nm), C-band (1530-1560 nm), and L-band (1560-1630 nm). Combined, these two windows provide a theoretical upper bound of 50 THz of bandwidth. The dominant loss mechanism in good fibers is Rayleigh scattering, while the peak in loss in the 1400 nm neighborhood is due to hydroxyl ion (OH-) impurities in the fiber. Other sources of loss include material absorption and radiative loss. Besides traditional fibers, full-spectrum fiber has also attracted a lot of attention in the industry, because of its permanently reduced water peak, as well as additional enhanced specifications in the L-band. Full-spectrum applications involve simultaneous (WDM) transmission in multiple operating windows (1270 to 1610 nm) over a single fiber. Full-spectrum fibers provide more useable wavelengths than standard single-mode fiber and therefore more bandwidth per fiber [17]. Specifically, low-water-peak fibers have attenuation specifications in line with the attenuation values in other transmission windows. Fibers with low-water-peak attenuation may use the 1360 to 1480 nm range without the severe loss previously experienced in traditional standard single-mode fibers. Industry standards organizations have

established new classes of standard single-mode fibers that require the average attenuation at 1383 nm after hydrogen aging to be less than or equal to the specified attenuation at 1310 nm.

1.3.1 Single Mode Fiber Vs Multimode Fiber

The total internal reflection may occur for any angle core angle which is greater than critical angle, light will not necessarily propagate for all of these angles. For some of these angles, light will not propagate due to destructive interference between the incident light and the reflected light at the core cladding interface within the fiber. For other angles of incidence, the incident wave and the reflected wave at the core-cladding interface constructively interfere in order to maintain the propagation of the wave. The angles for which waves do propagate correspond to modes in a fiber. If more than one mode may propagate through a fiber, the fiber is called multimode. In general, a larger core diameter or higher operating frequencies allow a greater number of modes to propagate. Fig 1.11 shows cross section view of single mode and multimode fiber.

The advantage of multimode fiber is that its core diameter is relatively large; as a result, injection of light into the fiber with low coupling loss can be accomplished by using inexpensive, large-area light sources, such as light-emitting diodes (LEDs). The disadvantage of multimode fiber is that it introduces the phenomenon of intermodal dispersion. In multimode fiber, each mode propagates at a different velocity due to different angles of incidence at the core-cladding boundary. This effect causes different rays of light from the same source to arrive at the other end of the fiber at different times, resulting in a pulse which is spread out in the time domain. Intermodal dispersion increases with the propagation distance [3].

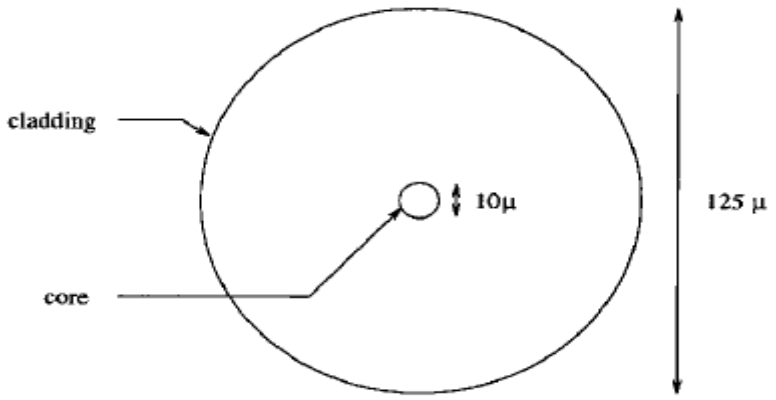

Fig 1.11 (a) Single-Mode Optical fiber

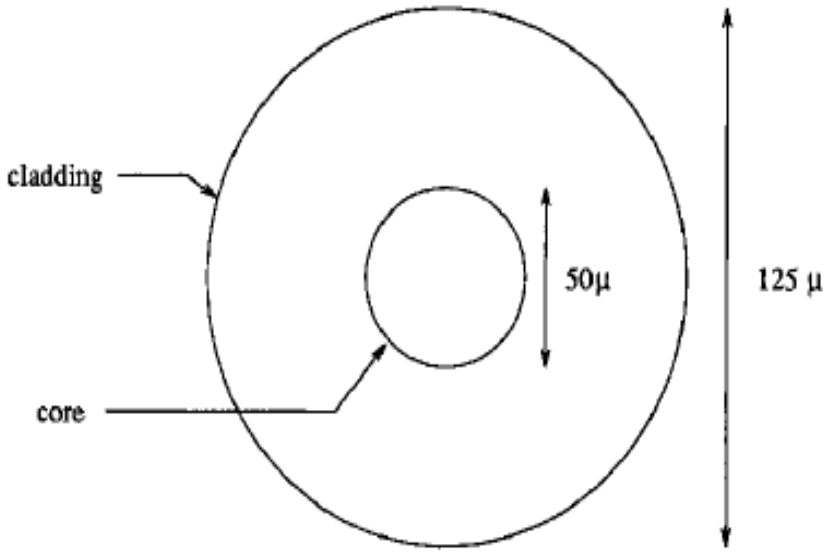

Fig 1.11 (b) Multimode Optical Fiber

1.4 Introduction to OptSim

The core version of OptSim was first developed in 1983 by the Optical Communication Group of Politecnico di Torino . The optical simulation software was originally known as TopSim, a transmission system simulation package, which was developed for mobile and satellite communication. TopSim was furthered improved with the addition of a library for optical systems and after continuous refinement efforts by the simulation specialists of Politecnico di Torino, the simulation software was later known as OptSim. OptSim is an advanced vectorial fiber simulator tool that takes into account all important phenomena including fiber loss, chromatic dispersion, birefringence, polarization mode dispersion (PMD), Kerr non-linearity and amplified spontaneous emission accumulation. OptSim is one of the two high-end commercial system simulators that are capable of calculating more than 15,000 km of non-linear fiber with high precision in a reasonable time. The fiber is simulated by solving the nonlinear Schrodinger equation using a modified version of the standard Split-Step Fourier (SSF) method, which solve the problems related to the cyclical numerical convolution effects intrinsic to the standard SSF method by implementing a true linear numerical convolution by means of component processing techniques (overlap-and-add algorithm). This method has allowed extremely long fiber links to be simulated on a large window (thousand of bits at standard bitrates) with excellent accuracy. OptSim is actually the fastest simulator because all the simulation components are based on a time domain computation [18]. With OptSim, it is possible to model very closely a “real” ultra-long haul system and achieve realistic results. In addition, continuous refinement of the design

parameters can be performed to achieve optimal results, which is difficult to perform in the hardware implementation environment because it can be costly, time consuming and relatively inflexible.

1.4.1 System Requirements

OptSim can be run on both the Unix and Windows NT platforms. The optical simulation software can be installed on any intel-based PC and the hardware requirements are as follow:

- Pentium II 400 MHz.
- Minimum of 64 Mbytes of RAM for data processing. 128 Mbytes of RAM for faster processing time.
- 100 Mbytes of free space for complete OptSim installation.
- A PostScript compatible printer to print the schematics or graphs created with OptSim.
- A Color graphic display with resolution of 1024x768 pixels or higher.

1.4.2 Simulation

OptSim provides multiple simulation engines that provide complementary simulation techniques. This enables the greatest flexibility in modeling and simulating systems ranging from short-distance data communication links, to ultra long-haul DWDM telecom systems, to large metro networks with feedback paths and EDFA transients due to adding and dropping of channels.

1.4.3 Analysis

Data Post-Processing and Display OptSim's data post-processing and display facilities provide an intuitive and flexible measurement graphical interface that acts as a lab like set of virtual instruments. Interactive and post-processing functionality (e.g. graph superimposition, correlation graphs, interactive cursor read-out data, peak search, eye-diagram measurements, BER/Q evaluation) allow one to simulate the project once and perform further analysis of results later (saving time during the design process).

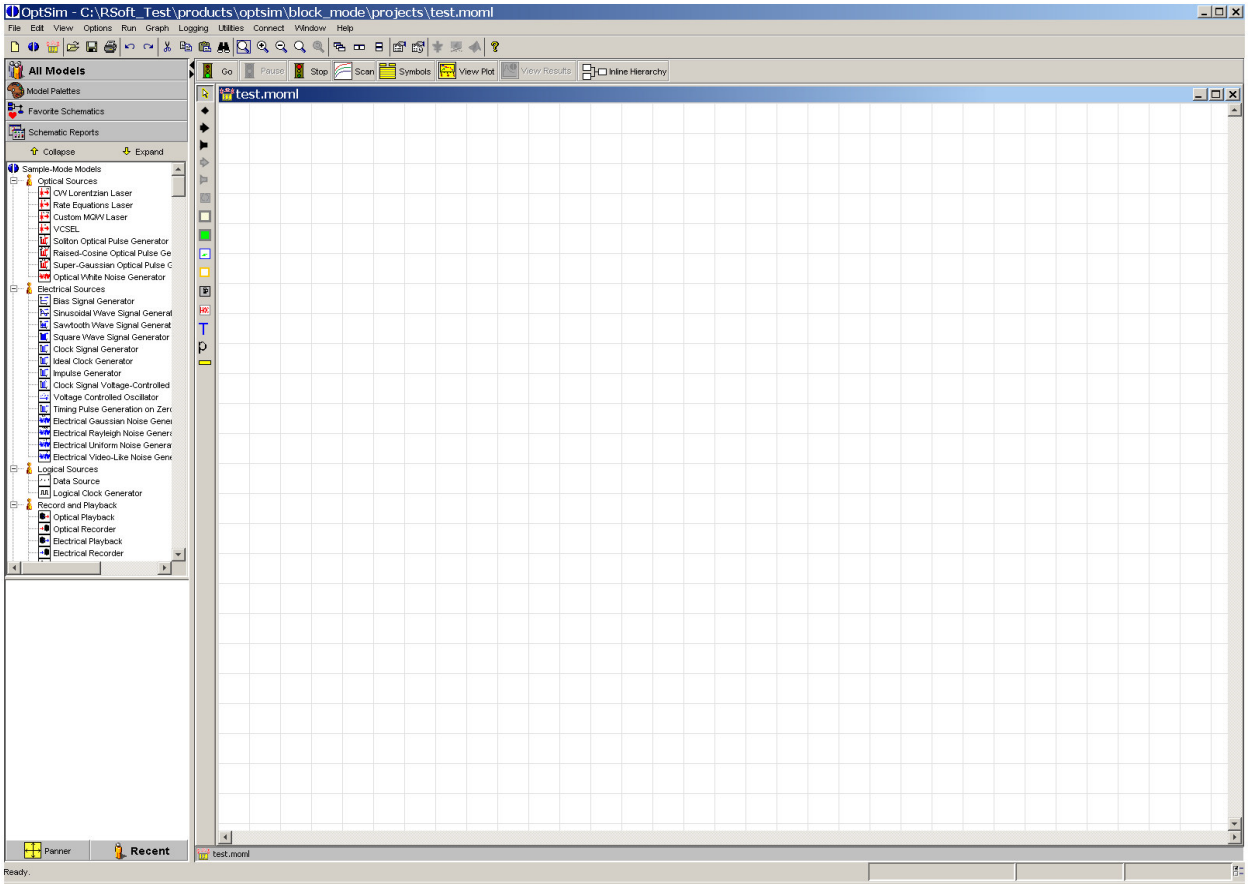

Fig 1.12 The OptSim graphical editor

Simulation results can be plotted in a number of forms including signal waveforms, eye diagrams, signal spectra, OSNR, Poincare sphere, dispersion maps and more. A wide and complete choice of measurements is available including jitter, eye opening/closure, electrical/optical spectra, chirp, optical instantaneous phase/frequency and power.

1.5 Modulation Formats

The ASK-based modulation formats are characterized by simple signal generation and detection, due to which all currently deployed optical transmission systems employ ASK-based modulation formats. The two basic modulation formats of are non-return- to-zero (NRZ) and return-to-zero (RZ).

1.5.1 Non-return-to-zero (NRZ) Modulation format

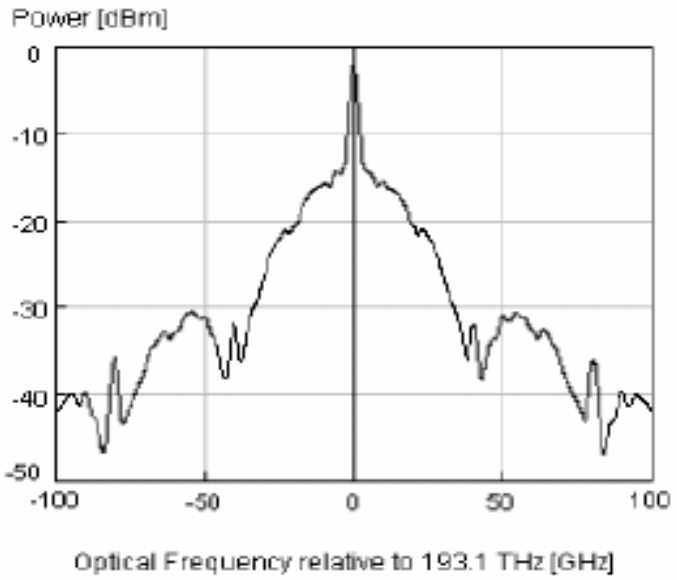

Fig 1.13 Optical spectrum of NRZ modulation format [19]

The simplest modulation scheme is a non-return-to-zero (NRZ) format, where the pulse is on for the entire bit period. Most commercial systems use the NRZ modulation format [18]. The non-return-to-zero (NRZ) has been the most dominant modulation format in intensity modulated-direct detection fiber-optical communication systems for the last years. The reasons for using NRZ in the early days of fiber-optical communication as it is not sensitive to laser phase noise, requires a relatively low electrical bandwidth for transmitter and receivers compare with RZ and the simplest configuration of transmitter and receiver. The NRZ pulses have a narrow optical spectrum as shown in figure (1.13). The reduced spectrum width improves the dispersion tolerance but it has the effect of intersymbol interference between the pulses this modulation format is not suitable when high bit rates and distance are considered. The narrow spectrum of NRZ pulses yields a better realization of dense channel spacing in DWDM systems.

1.5.2 Return-to-zero (RZ) modulation format

In return-to-zero (RZ) modulation format, power is transmitted only for a fraction of the bit period. A RZ signal with the same average power of a NRZ signal has a spectrum peak-power twice larger than the NRZ pulse. The main characteristic of RZ modulated signals is a relatively broad optical spectrum. The large spectral width results in a reduced dispersion

tolerance and a reduced spectral efficiency of RZ- based systems. The RZ pulse shape enables an increased robustness to fiber nonlinear effects and to the effects of polarization mode dispersion (PMD) [20]. The RZ system implementation improves the system receiver sensitivity up to 3 dB [19]. Due to its broader spectrum, RZ pulse has a reduced dispersion tolerance and spectral efficiency. The duty cycle of RZ pulse is less than unity. The reduced pulse width implies a broader signal spectrum making this technique less interesting for the implementation in DWDM and other communication systems. The RZ modulation format is used for long haul optical communication systems working at higher bit rates. . The RZ pulse optical spectrum is shown in figure 1.14.

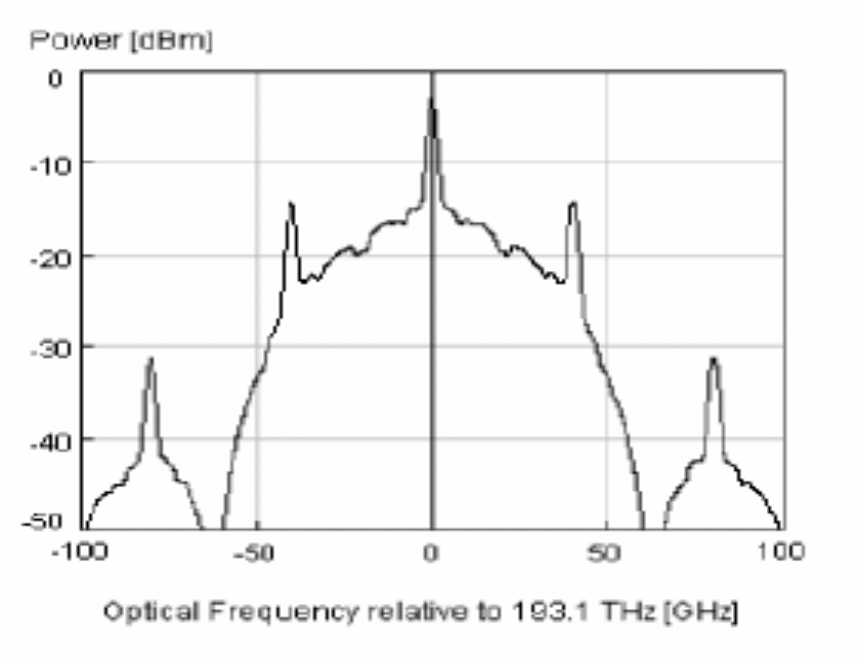

Fig 1.14 Optical spectrum of RZ modulation format [19]

1.6 Thesis Objective

In optical communication systems, the key component on the transmitter side is light source. Today semiconductor lasers are widely used as optical source at due to capability of operating at single mode and very narrow beam width. The operation of any device depends upon operating conditions in which it is operated. For reliable communication, effect of environmental conditions should be known that affect the operation of the laser. The behaviour of transmitted signal at the receiver side depends upon the media of communication, distance from transmitter and format in which it is transmitted. Different

optical fibers behave differently, to the laser output which is modulated by various modulators and coding formats. **The key objective of this thesis is**

1. **To study the effects of change in ambient temperature of VCSEL in terms of output optical power and propagation of VCSEL signal through single mode and multimode fibers.**
2. **To study the effect of bias current on output optical power of DFB laser in terms of output optical power and output optical spectrum.**
3. **To evaluate the performance of different coding formats and modulation techniques using DFB laser with the variation of link length of the optical system in terms of propagation distance, BER and Q factor.**

1.7 Thesis Organization

This chapter includes the brief introduction to the optical communication with brief history. In this VCSEL, DFB laser, modulation formats are discussed in brief. The **Second chapter** contains the literature survey about effect of temperature on VCSEL output, optimization of DFB laser bias current, RZ and NRZ modulation formats on optical communication. In the **third chapter,** the effects of temperature variation and propagation of VCSEL signal through single mode and multimode fiber are studied with the help of eye diagrams, optical spectrum and power output. The **fourth chapter** contains the optimization of DFB laser bias current; this is optimized with the help of eye diagrams, output optical spectrum at different bias current values. Using the optimized bias current impact of modulation schemes and formats is studied. Finally the **fifth chapter** gives the conclusion and future work of the thesis.

Chapter-2 Literature Review

The behaviour of semiconductor lasers is very important to understand, for a reliable communication system. The work done by different authors is reviewed is given below.

N. Nishiyama et al. [21] gave their ideas about 1.3 μm and 1.55-μm vertical-cavity surface-emitting lasers (VCSELs) on InP. High-reflectivity AlGaInAs–InP lattice matched distributed Bragg reflectors (DBRs) were grown on InP substrates. 1.7 (for 1.3 μm) and 2.0 (for 1.55 μm) mW single mode power at 25 °C, 0.6 mW single mode power at 85 °C and lasing operation at >100 °C have been achieved. 10 Gbit/s error free transmissions through 10 km standard single mode fiber for 1.3-μm VCSELs, and through 15 km nonzero dispersion shift fiber for 1.55-μm VCSELs, had been demonstrated. With the addition of an SOA, 100 km error free transmission at 10 Gbit/s also has been demonstrated through a negative dispersion fiber. No degradation has been observed after over 2500-h aging test.

Adil Karim, Joachim Piprek et al. [22] reported on the fabrication and operation of the first electrically pumped 1.55 μm vertical-cavity laser array for wavelength-division-multiplexing applications. The array consisted of four channels operating between 1509 nm and 1524 nm. Wafer bonding was used to integrate GaAs–AlGaAs distributed Bragg reflectors with an InP–InGaAsP active region.

Mikihiro Kajita, Takeshi Kawakami, Masaaki Nido et al. [23] reported that emperature-insensitive characteristics are of great importance in implementing the actual applications of vertical cavity surface-emitting lasers (VCSEL's) because of the temperature change in the surroundings. To extend the operational temperature range of such lasers, they fabricated a VCSEL with a broad gain bandwidth. The active layers in VCSEL's consist of multiple quantum wells (MQW's) with different bandgap energies. From the change in the threshold current, with temperature as a parameter, they found that the operational temperature range of a VCSEL with a broad gain bandwidth is more than 20 °C wider than that of conventional VCSEL's, whose active layers consist of a single type of MQW. They demonstrate that the extended-gain bandwidth gives better temperature characteristics. In addition, they presents

simulated the structure of the active layers, and the optimized structure resulted in a 1-mW light output power at less than 5 mA in a single transverse mode oscillation from 20-70 °C.

J. J. Morikuni, K. W. Wyatt et al. [24] presented a simple thermal model of vertical-cavity surface-emitting laser (VCSEL) light-current (L-I) characteristics based on the laser rate equations and a thermal offset current. The model was implemented in conventional SPICE-like circuit simulators, including HSPICE, and used to simulate key features of VCSEL L-I curves, namely, thermally dependent threshold current and output-power roll-over for a range of ambient temperatures.

Keun Ho Rhew, Dae Hee Lee et al. [25] studied the long-term reliability of all monolithic 1.55 μm etched-mesa vertical cavity surface emitting lasers (VCSELs) with tunnel junction via high-temperature storage tests and accelerated life tests. They presented characteristic variations depend on the operating conditions are examined via the threshold current, the optical output power, and the dark current. The activation energy of the VCSELs is calculated based on the reliability testing results. In addition, the degradation mechanism of the tested VCSELs is analyzed using the correlation between the current–voltage characteristics (I–V) and the device lifetime. From these results, the long-term reliability of the VCSEL test structures for high-speed optical communication systems can be determined and the device parameters, such as dark current, can be used as a monitoring factor for estimating reliability of the VCSELs.

Robert **A.** Morgan [26] presented the progress in elimination of the excessive voltage-drop that plagued VCSELs. Threshold voltages as low as Vth = 1.53 V are now commonplace. Operating voltages, current and powers are typically, < 1.8V, ≅ 10mA and > 1mW. Even submilliamp threshold currents (I_{th} = 0.68 mA) had been demonstrated with this planar all-AlGaAs structure. Moreover, continuous wave power greater than 59 mW, and respectable had been demonstrated. VCSEL robustness is presented by maximum cw lasing temperature T = 200 °C, and temperature ranges of 10K to 400K, and -50 °C and 155 °C on a single VCSEL.

N. Laurand, S. Calvez et al. [27] analyzed the 1.55 μm pulsed operation of an optically-pumped GaInNAsSb vertical-cavity surface-emitting laser (VCSEL). The structure employs a

dielectric (SiO_2=TiO_2) top mirror, while the bottom mirror and active region were grown on GaAs by MBE. Temperature dependent (10°C–40°C) laser measurements were made.

Feng-Ming Lee, Chia-Lung Tsai et al. [28] investigated and characterized the 1.3-μm single-mode vertical-cavity surface-emitting lasers (VCSELs) with two GaInAsN strained multiple quantum wells as the active region. Surface relief technique and a thick silicon oxide were used for the spatial mode filtering and the planarization processing, respectively. The VCSELs with a 5-μm-diameter surface-relief aperture and a 12-μm-diameter oxide-confined aperture at room temperature exhibit a threshold current of 3 mA, a slope efficiency of 0.14 mW/mA, a maximum operation temperature of 90 ◦C, and a single-mode behavior. These VCSELs show a maximum light output power of 1 mW for the single fundamental mode with a transverse-mode suppression of more than 30 dB and also show a clear eye-opening feature operated at 2.488 Gb/s and 12.6 mA.

Yoshitsugu Wakazono, Katsuya Kikuchi et al. [29] presented the influence of higher-order mode of VCSEL emission on the coupling efficiency between VCSEL and waveguide. Firstly, they measured and simulated the coupling efficiency between VCSEL and step index multi mode fiber and pointed out the influence of higher-order of VCSEL emission and then measured the VCSEL power intensity and analysed the dependency of higher order transverse-mode of VCSEL emission numerically. They revealed that the fundamental transverse mode shared only 10-20% of actual VCSEL power emission.

Melanie Ott [2] presented, high temperature testing is used to determine LED and laser diode lifetimes, even though laser diode failure mechanisms are more sensitive to increases in current density. He presented that the current density is of great significance when searching for failure modes in a laser diode. The reliability of semiconductor sources is very dependent on the degradation modes.

S. F. Yu [30] gave quasi-three-dimensional dynamic model of index guided vertical-cavity surface-emitting lasers. Detailed structure of Bragg reflectors and lateral optical confinement were considered into the model. A three-dimensional waveguide problem is reduced to one dimension by using the effective index method. The dynamic response of optical field is solved by the time-domain algorithm. In addition, the lateral variation of carrier

concentration, refractive index, and spontaneous-emission profile are also determined in a self-consistent manner. Using this model, the influence of carrier transport and hot carriers on the dynamic behaviour of vertical-cavity surface-emitting lasers is studied. They found that these nonlinearities have significant influence on the relaxation-oscillation frequency and modulation bandwidth of the devices.

A. Mohd Sharizal et at. [31] studied the oxide-confined vertical-cavity surface-emitting lasers (VCSELs) operating in the 850 nm region of the electromagnetic spectrum. In this regard, various relevant VCSEL samples with numerous oxide aperture sizes had been fabricated and characterized. They reported that the VCSELs with oxide aperture size <10 µm require low threshold currents (<1 mA). Further, the differential quantum efficiencies up to 28% corresponding to wall-plug efficiencies of up to 15% were measured for a number of these devices.

A.A. Dyomina, V.V. Lysak et al. [32] investigated the thermal dependence of mirror reflective properties in oxide-confined vertical-cavity surface-emitting lasers. The temperature distribution over a cavity versus applied current was calculated. The refractive indexes of the mirror layers were subsequently redefined using the temperature coefficients, and changes in radial reflectance spectra of the mirror were analysed. Results show a shift of stop-band and Bragg wavelengths of the mirror, as well as a shift of laser operation wavelength at different injection currents and the formation of a temperature lens in the mirror due to a decrease in temperature close to the edge of the oxide windows.

Michel Krakowski, Daniel Rondi et al. [33] presented GalnAsPlnP distributed feedback (DFB) buried ridge structure laser diodes emitting at 1.52 µm. They found that the minimum CW threshold current of 5 mA is the lowest yet reported for DFB lasers at 1.5 µm. Single longitudinal mode operation with a side mode suppression ratio of 40 dB from 20 to 100°C had been obtained At only 20 mA above threshold, a bandwidth of 9.6 GHz and a relative intensity noise (RIN) lower than - 150 dB/Hz at 4 GHz have been measured.

G.F.Barlow and K.A.Shore [34] gave an analysis of a circular grating organic semiconductor distributed feedback laser operating at 632 nm. Threshold current calculations were undertaken using gain coefficients for the Alq3: DCM lasing material employed. It was

shown how variations in the radii of the inner and outer sections of an annular grating may be expected to affect threshold characteristics.

Manoj Kumar et al. [35] presented the comparative investigation and suitability of various data formats for optical soliton transmission linksat10Gb/s for different chirps (-0.7 to 0.7). Here the investigations focused on data formats: NRZ, RZ soliton, RZ raised cosine and RZ super Gaussian. The comparative results and suitability of data formats is based on various performance measures such as Q-factor, eye opening, BER and jitter. It had been indicated that RZ super Gaussian yields the highest value of Q (34.08 dB), good eye opening and lowest BER.

Aihan Yin, Li Li Xinliang Zhang [36] presented three different modulation formats including non return-to-zero, return-to-zero, carrier-suppressed return-to-zero and the differential phase keying modulation format of each code. A method of their modulated signal generation with computer was described, and a comparison of their spectra and waveforms was made. The 40Gbps signal transmitted in 200 km G.652 fiber by way of single channel with erbium-doped-fiber-amplifier is simulated for these three formats. The ability of anti-dispersion and anti-polarization mode dispersion was analyzed. It was shown that return to zero and carrier-suppressed return-to-zero formats are more tolerant than non return to zero format in the same conditions.

Chapter-3 Performance evaluation of VCSEL at various physical parameters and propagation through single and multi mode fibers

3.1 Abstract

This chapter presents influence of the change in temperature of a vertical cavity surface emitting laser (VCSEL) on its output power. It is observed that with increase in temperature of laser its output power decrease. It is also observed that with decrease in threshold voltage of the laser output power increase. Decrease in output power due to increase in temperature can be compensated by increasing driving current. But increase in drive current decrease life of the laser. So a laser with lower threshold voltage can be used to operate at high temperature with long life. Propagation of VCSEL through single mode and multimode fiber is also studied. In single mode fiber only one propagation mode exists due to which signal can be transmitted to longer distances.

3.2 Introduction

Vertical cavity surface-emitting lasers (VCSEL's) are being developed as a light source for optical interconnections. VCSEL's enable many types of applications, such as optical computing and optical information processing [37]. VCSEL's have such unique advantages as a small size single longitudinal mode, due to the short cavity length, ease in forming a two-dimensional (2-D) array, low power consumption, and a small light beam divergence. Recent years have brought about great improvements in such basic characteristics as the slope efficiency, threshold voltage and light output power [38]. In some applications, VCSEL's are to be used without a temperature control circuit, in which case it is important that the VCSEL be temperature-insensitive [39]. Because the cavity mode shifts at a rate of 0.07 nm/°C, and the gain peak shifts at a rate of 0.3 nm/°C, the cavity mode is not aligned with the gain peak as the temperature increases. This reduces the light output power and increase the drive current [40].

An increase in temperature is caused by a) self heating, b) thermal crosstalk in simultaneous operation of array devices, and c) changes in ambient temperature. One way to prevent a) and b) is to reduce the electrical series resistance of the device to decrease heat generated in

simultaneous oscillation of array devices. VCSEL's have a higher electrical series resistance than edge-emitting lasers because current is injected through highly resistive DBR's [41].

P. V. Mena and J. J. Morikuni [24] presented a simple thermal model of vertical-cavity surface-emitting laser (VCSEL) in which they presented thermally dependent threshold current and output-power roll-over for a range of ambient temperatures. They showed that if the input current is constant and temperature is increased output power of the laser decrease. N. Nishiyama, C. Caneau and B. Hall [21] presented the effect of cavity length, temperature on output power of the laser. They concluded that with increase in cavity length of the laser output power increase. But increase in temperature results decrease in output power of the laser. Decreasing the defects in the active region as well as decreasing the threshold current is important for obtaining a long-lifetime VCSEL [42].

According to [24], [21] the output power can be compensated by increasing the driving current of the laser. But increasing the operating current limits the life of laser.

In this chapter we study the effect of variations in threshold voltage on output of the laser. Observations are made by varying the temperature. Propagation of VCSEL output from single mode and multimode fibers is also studied. It is observed that there is decrease in output power with increase in temperature and to compensate this if threshold voltage is decreased there is significant rise in output power of the laser.

In section 3.1 abstract of the work done in this chapter is given, section 3.2 discuss the factors which are responsible for heating and how it affects the operation of laser. Section 3.3 describes the simulation setup using OptSim. In section 3.4 results obtained in simulation are presented and finally conclusions are discussed in section 3.5.

3.3 Simulation Setup

To investigate the temperature dependent performance of the VCSEL an Optical and Electrical Transmission Systems Design & Simulation Environment based OptSim tool is used. Setup for analysing the effect of temperature is shown in figure 3.1(a). A shown in figure data source generates data at 2 Gb/s which is converted into NRZ Raised Cosine format by signal driver with low level 0.005 V and high level 0.03 V. This driver drives VCSEL laser operating at 1550 nm and signal is modulated directly in the laser cavity. After modulation laser output optical power travel through ideal optical fiber. This signal is splitted with the help of splitter and fed to power meter and optical receiver separately. Output optical

power is measured with the help of power meter. Receiver detector is PIN photodiode with quantum efficiency 0.5599 and responsivity 0.7 A/W. After detection it is passed through electrical filter which is of type raised cosine with bandwidth of 1 GHz this filtered signal is analysed with the help of electrical scope and Q estimator.

To investigate the laser behaviour temperature of laser is varied. Then output in plotted against temperature. To compensate temperature effect on the output of the laser a compensating parameter threshold voltage of the laser is varied. Then output power is plotted as function of threshold voltage.

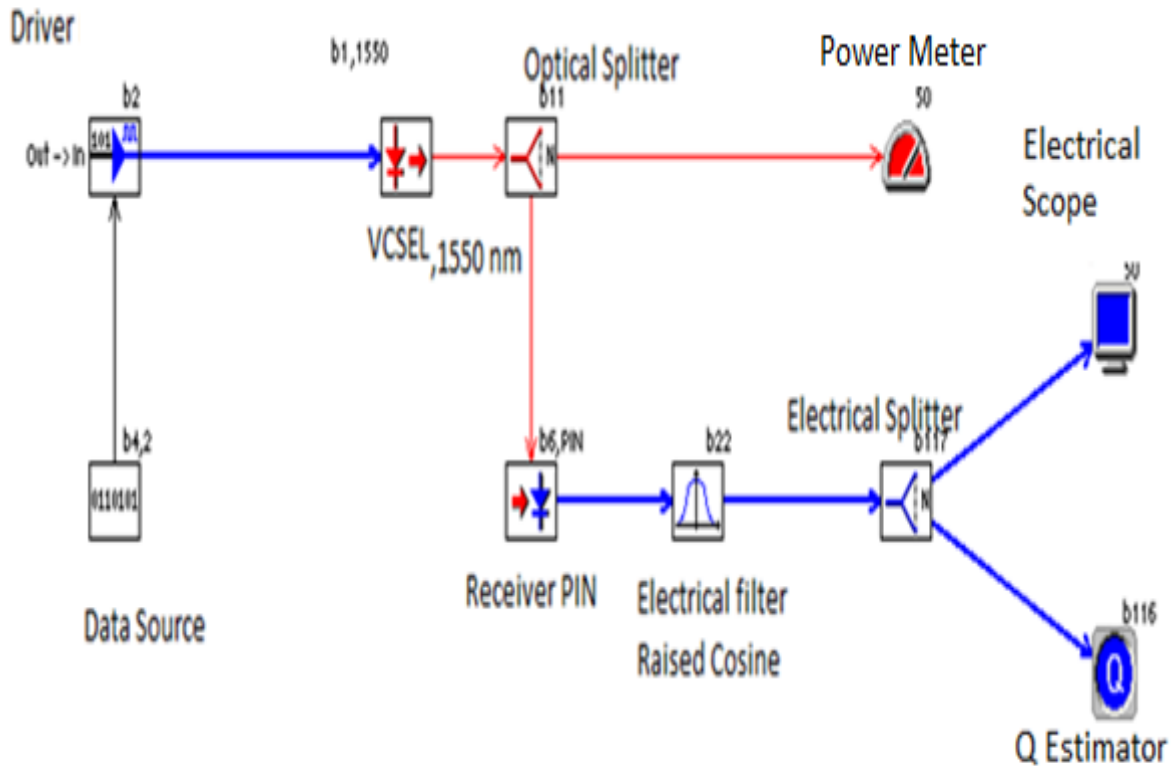

Fig 3.1 (a) Setup for analysing the effect of temperature

For analysing the propagation of VCSEL signal through single mode and multimode fiber setup is shown in figure 3.1 (b). Components used here have same parameters used in setup 3.1 (a). It uses single mode fiber with attenuation 14.4 dB/km and multimode fiber with same value of attenuation. Here data generated by data source at 2Gb/s and is made to travel through these fibers. Length of multimode fiber is varied from 50m to 250m and length of SM fiber is varied from 500m to 4 km. The signal is analysed with the help of power meter, electrical scope and Q estimator.

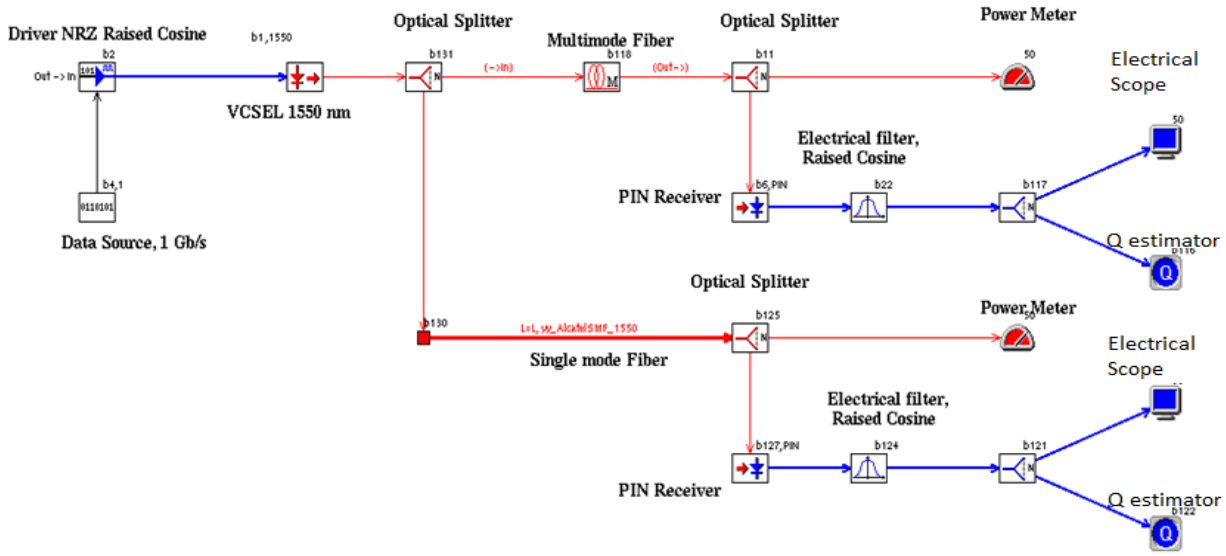

Figure 3.1 (b) Setup for Propagation through SM and MM fiber

3.4 Result and discussions

In the previous sections, we discussed various components used in the simulation setup. Using this setup the measurements of output power by varying the temperature from 20°C to 70°C are taken. This is shown in figure 3.2.

It is observed that with rise in temperature there is significant decrease in output power level of the laser. This limits the applications of the laser to operate at high temperatures.

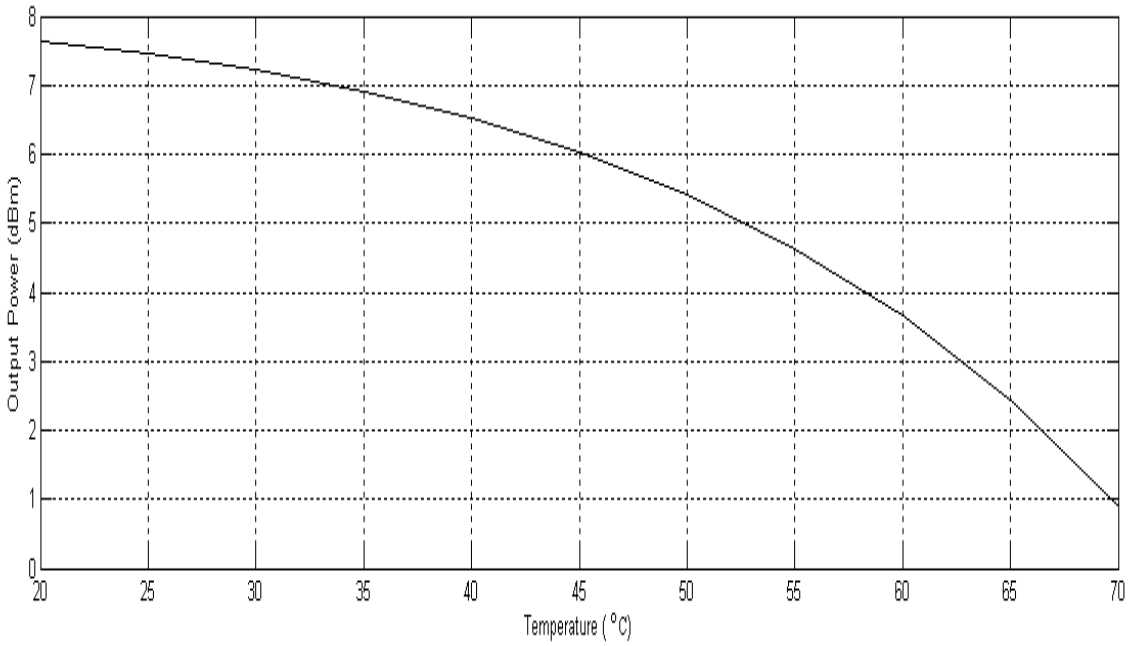

Figure 3.2 Temperature Vs Output Power

With change in threshold voltage of laser there is significant change in output optical power. Threshold voltage is changed from 1.4 V to 1.75 V keeping the temperature constant. These observations again show that output of laser is function of threshold voltage and operating temperature.

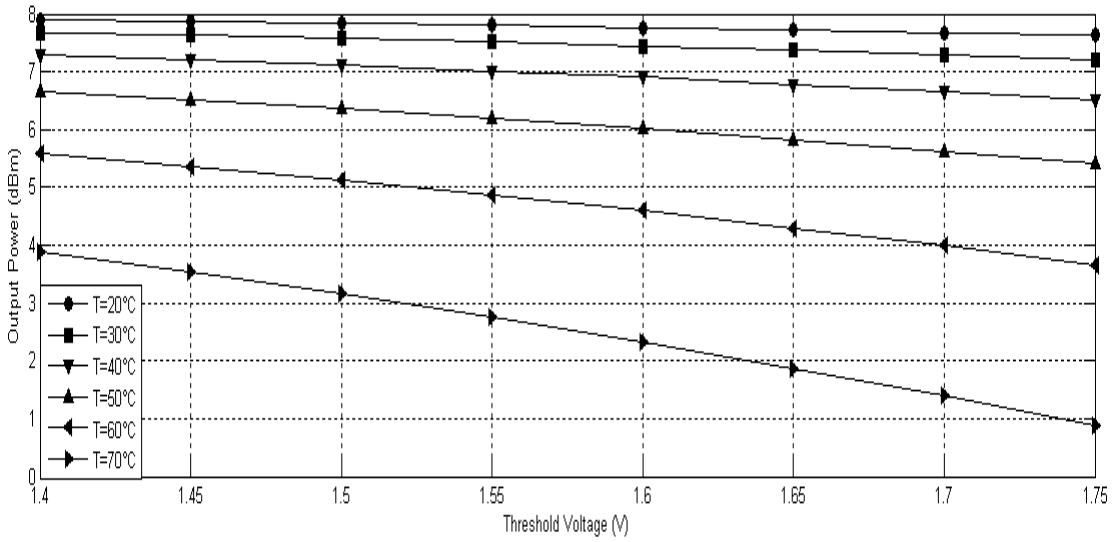

Fig 3.3 Threshold voltage Vs Output Power

If threshold voltage decreases corresponding output power of laser increases. If temperature increases corresponding output power of laser decreases. These two factors oppose each other. Variation of output with respect to threshold voltage is shown in figure 3.3.

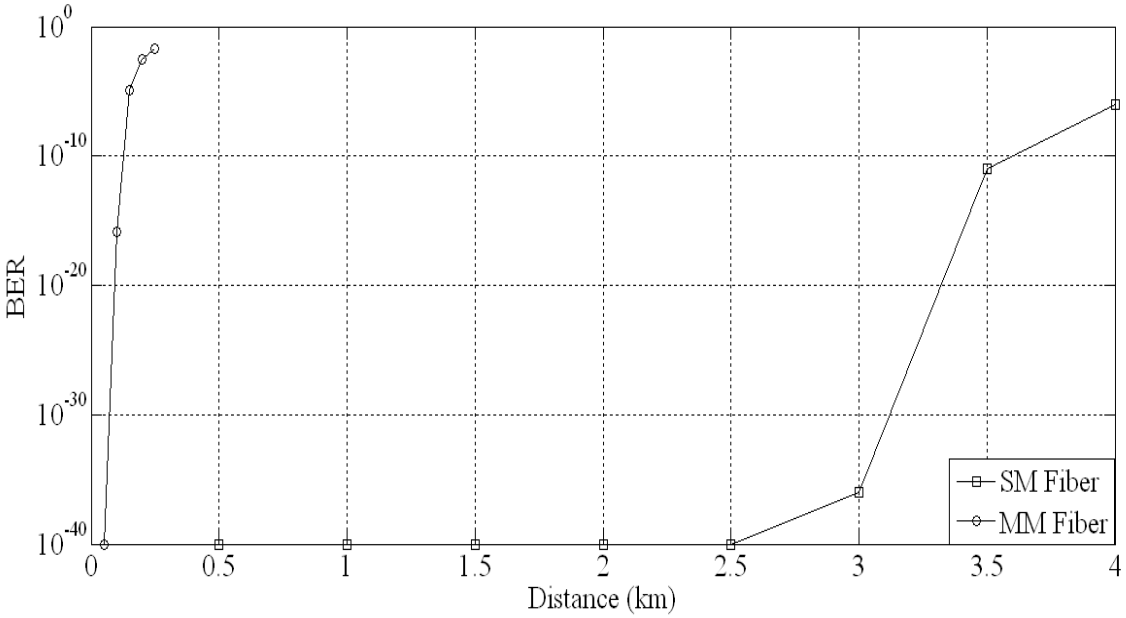

Fig 3.4 Distance Vs BER

The figure 3.4 shows the bit error rate with variation of length of fiber. The distance is varied from 50m to 250m in five steps for MM fiber and 500m to 4km for SM fiber. It is observed that there is sharp increase in bit error rate of multimode fiber with short distances but on the other side single mode fibers can transmit to longer distance as compared to multimode fibers.

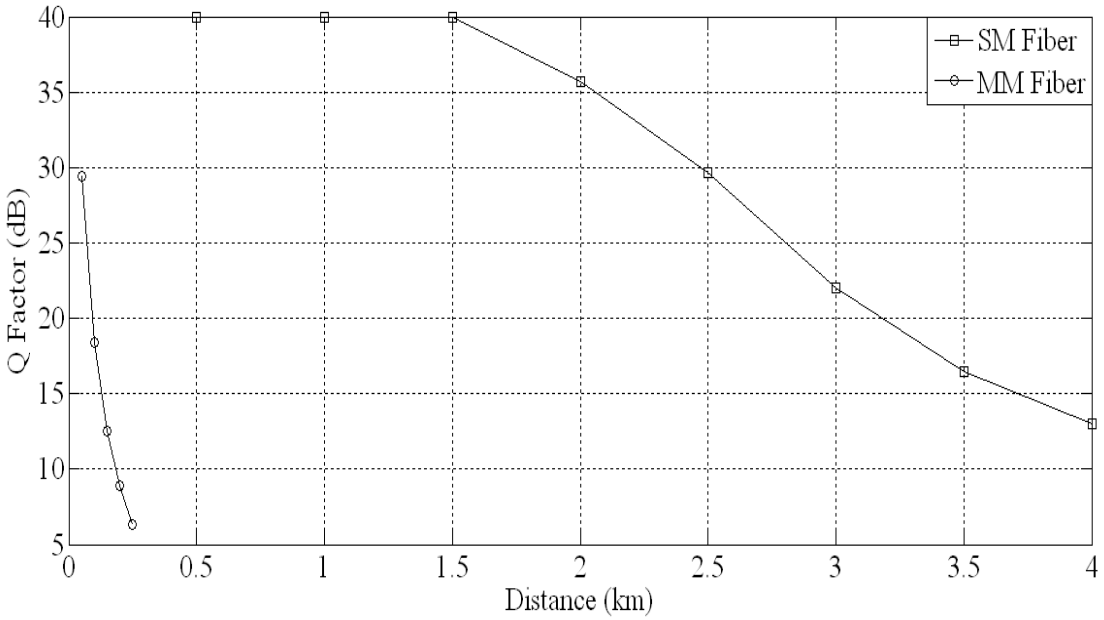

Fig 3.5 Distance Vs Q factor

Figure 3.5 shows variation of Q factor as function of distance. It is observed that Q-factor decrease sharply for multimode fiber only for short distance.

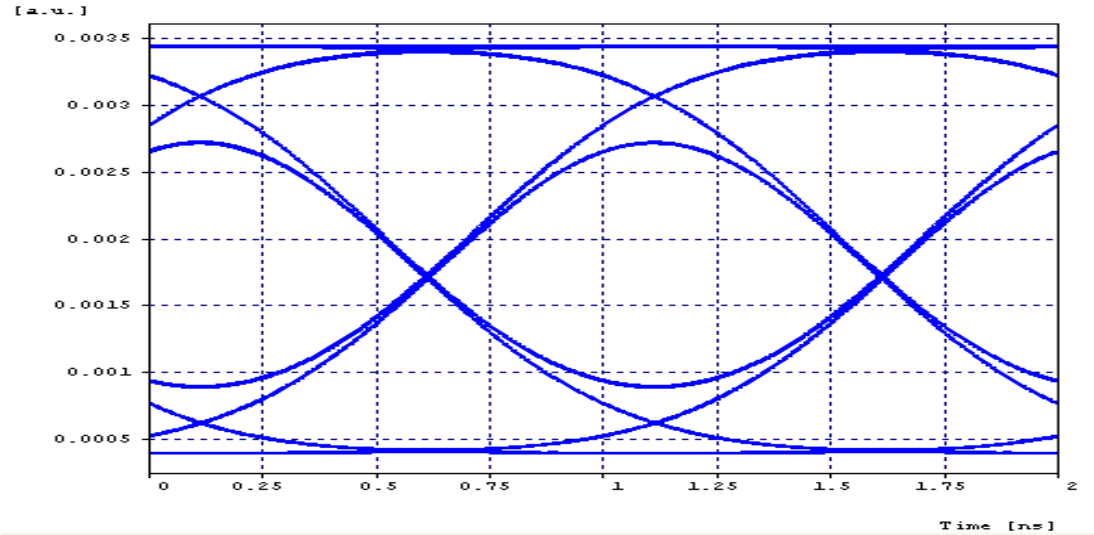

Fig 3.6 Eye Diagram for MM fiber at 125m With BER 10^{-9}

The eye diagram for multi mode fiber is shown in figure 3.6. The eye diagram shows that minimum bit error rate is achieved up to 125m.

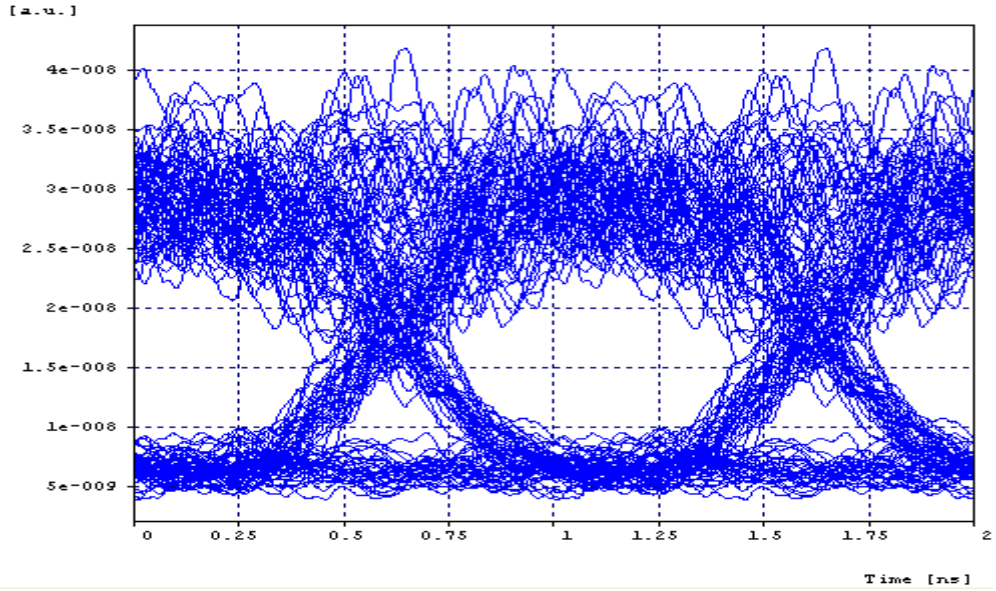

Fig 3.7 Eye diagram for SM fiber at 3.7 km with BER 10^{-9}

The eye diagram for single mode fiber is shown in figure 3.7. The eye diagram shows that minimum bit error rate is achieved up to 3.7 km.

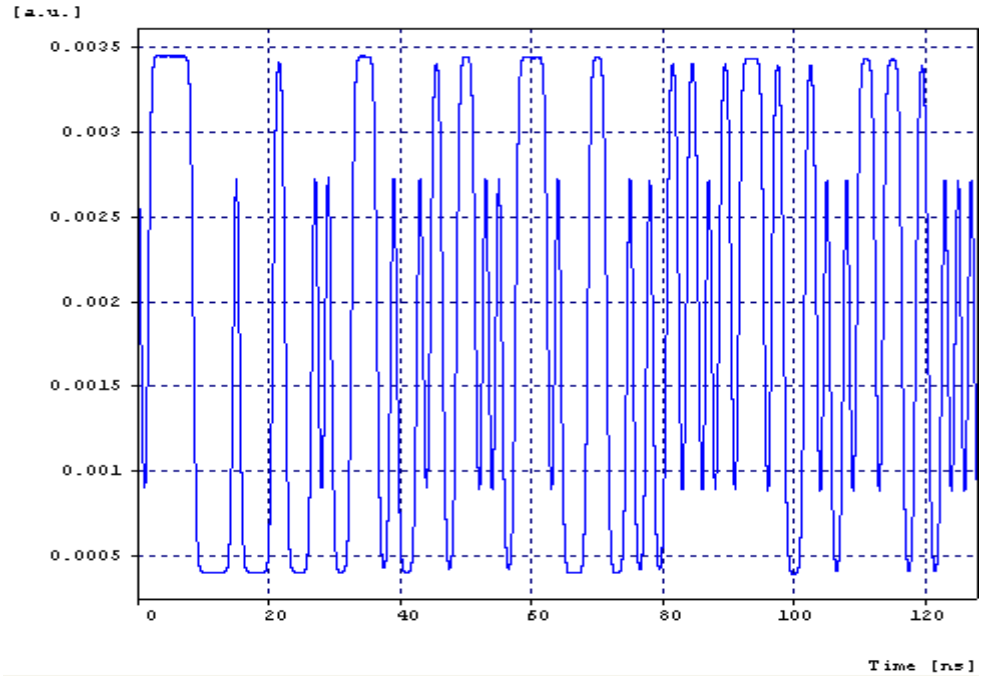

Fig 3.8 Output signal for MM fiber at 125 meters

The output power signal for multi mode fiber is shown in figure 3.8. This diagram shows that system gives acceptable output power signal up to 125m.

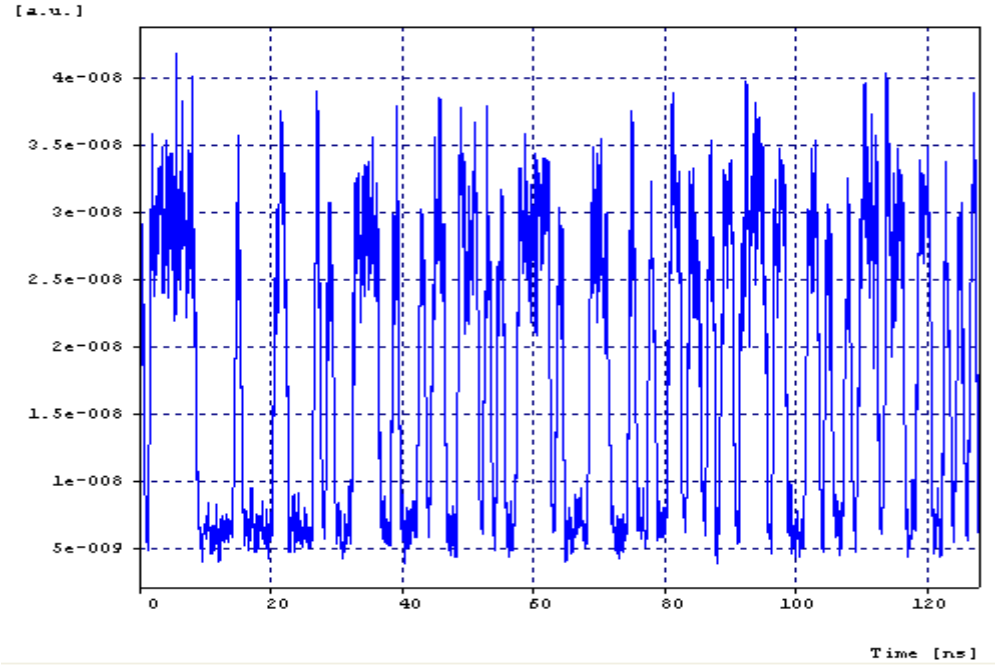

Fig 3.9 Output signal for SM fiber at 3.7 km

The output power signal for single mode fiber is shown in figure 3.9. This diagram shows that system gives acceptable output power signal up to 3.7 km.

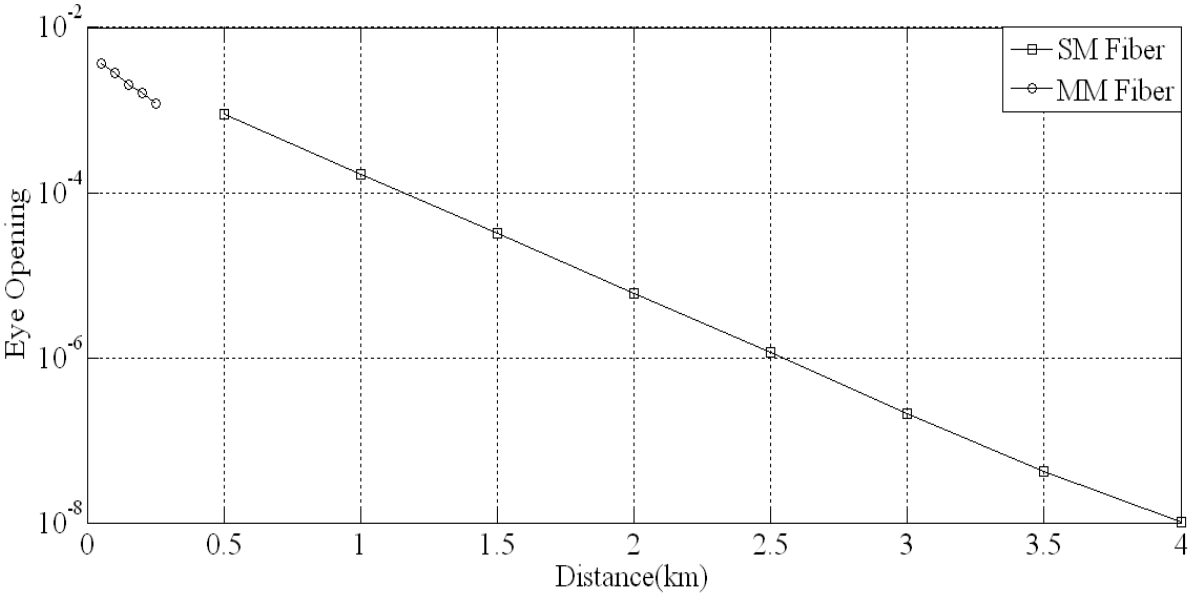

Fig 3.10 Distance Vs Eye opening

Figure 3.10 shows the comparison of output signal eye opening with distance. This comparison shows that eye opening is better in single mode fiber than multi mode fibers.

The performance of multi mode fibers is only up to 125 m while single mode fibers perform better up to 3.7 kms. So, for long distance, single mode fibers are best but for short distance multi mode fibers are better than single mode fibers.

3.5 Conclusion

It is concluded that the output of laser decreases with rise in temperature. This limits its operations at high temperature. But at the same time, decreasing the threshold voltage increases the output power of the laser. These two factors cancel out each other. So, to operate laser at high temperature, it should be designed with lower threshold voltage. Using VCSEL with multimode and single mode fiber, it is obtained that multimode fiber can transmit signal with acceptable BER of 10^{-9} up to small distance only. On the other hand, single mode fibers can transmit with same BER to larger distance. With same input power MM fiber can transmit signal with BER 10^{-9} up to distance of 125 meters. Whereas, SM fibers can transmit the signal with same BER up to 3.7 km.

Chapter 4 Performance evaluation of DFB laser using different modulation techniques and coding formats with the optimization of bias current

4.1 Abstract

In this chapter effect of bias current on DFB laser is studied. The laser is biased at bias current less than threshold, near threshold and above threshold. It is observed that when laser is biased at current very small than bias current output power is very low, at bias current near to threshold output power increase sharply. And at bias current greater to threshold output power increase less sharply, after certain value it get saturated. BER also decrease with increase in bias current up to 40 mA and remain at its minimum value up to 70 mA, after that it again starts increasing. It is observed that DFB laser with threshold current 15.37 mA gives best performance at 40 mA which is 2.6 times of the threshold current with BER 10^{-9} .The laser is biased at 40 mA and performance of return to zero and non return to zero data formats is studied by using amplitude and phase modulator. NRZ raised cosine give acceptabe performance using amplitude modulator up to 70 km and NRZ rectangular give same performance with phase modulator up to 90 km

4.2 Introduction

The role of optical source is to convert an electrical input signal into the corresponding optical signal and then launch it into the optical fiber serving as the transmission medium. The propagation of light through optical fiber depends upon type of modulation, output spectrum etc of the light source. The output spectrum depends upon the laser driving current. For better and reliable performance it should be optimized [43].

Nowadays distributed feedback (DFB) semiconductor lasers play a decisive role in high bit-rate optical communication systems. DFB semiconductor lasers are suitable candidates for future direct-detection and coherent-detection optical communication systems which require highly stable, narrow-line width, high-output-power laser sources [44].

DFB laser diodes do not use two discrete mirrors to form the optical cavity (as they are used in conventional laser designs). The grating acts as the wavelength selective element for at least one of the mirrors and provides the feedback, reflecting light back into the cavity to form the resonator. The grating is constructed so as to reflect only a narrow band of

wavelengths, and thus produce a single longitudinal lasing mode. This is in contrast to a Fabry-Perot Laser, where the facets of the chip form the two mirrors and provide the feedback. In that case, the mirrors are broadband and either the laser functions at multiple longitudinal modes simultaneously or easily jump between longitudinal modes. Altering the temperature of the device causes the pitch of the grating to change due to the dependence of refractive index on temperature. This dependence is caused by a change in the semiconductor laser's bandgap with temperature and thermal expansion. [45].

In most cases, the transmission is digital, making the system very versatile and relatively insensitive, e.g. to nonlinear distortions. There are various different modulation formats, i.e., different methods for encoding the information. For example, a simple non-return-to-zero (NRZ) format transmits subsequent bits by sending a high or low optical power value, with no gaps between the bits, and extra means for synchronization. In contrast, a return-to-zero (RZ) format is easily self-synchronizing by returning to a rest state after each bit, but it requires a higher optical transmission bandwidth for the same data rate [46].

C. Caneau, M. H. Hu et al. [21] calculated threshold current for various DFB laser structures experimentally and theoretically and analysed the performance of laser operating at threshold current.

James E.A. Whiteaway et al. [47] gave a detailed nonlinear model for the performance of single-frequency laser structures operating both below and above threshold. The output power from each end of the laser and the emission wavelength, and the longitudinal intensity, carrier density, and relative permittivity profiles are predicted as a function of drive current above threshold for each lasing mode. The line width is also estimated while allowing for the non uniform longitudinal distribution of spontaneous emission into the mode in a physical manner. Carlos A.F. Fernandes et al. [48] presented the effect of bias current on the lasing-wavelength, the emitted power and the side-mode suppression ratio. For $I=5\ I_{th}$, where I_{th} is the laser threshold current, substantial improvements are achieved in the proposed DFB laser. If a laser with threshold current 15.37 mA used in this paper is operated at bias current which is five times of the threshold current will degrade performance due to high current density.

In this chapter for the optimization of bias current of DFB laser, observations are made for different values above and below threshold current of laser with threshold current 15.37 mA. Optimization of RZ and NRZ coding formats using external amplitude and phase modulators is made using DFB laser which is biased at optimize bias current.

Section 4.1 gives abstract of work done in this chapter, section 4.2 gives brief introduction of laser and effect of variations in bias current and coding format is discussed. Section 4.3

describes the simulation setup using OptSim. In section 4.4 results obtained in simulation are presented and finally conclusions are discussed in section 4.5.

4.3 Simulation Setup

In this model 1550 nm DFB laser is drived at different values ranging from 1 mA to 90 mA. The output of the laser is fed to amplitude modulator. Data source generate data at the rate of 10Gb/s which is encoded into NRZ:Raised cosine format with the help of driver with low level -2.5 V and high level 2.5 V, this data is used to amlitude modulate the laser output. A DFB laser operating at 1550 nm with threshold current 15.37 mA, linewidth 17.50 Mz, field confinment factor 0.3 is used which is driven by bias current. Optical output power and output optical spectrum can be measured with the help of power meter and optical probe. After modulation the data travel through ideal optical fiber and is received by sensitivity optical receiver. This sensitive optical receiver use PIN diode as detector and electrical filter of type bessel PIN diode has quantum efficiency 0.75 and responsivity 0.9376 A/W. The signal is analysed with the help eye diagram, Q factor and BER are measured with the help of Q estimator and BER estimator.

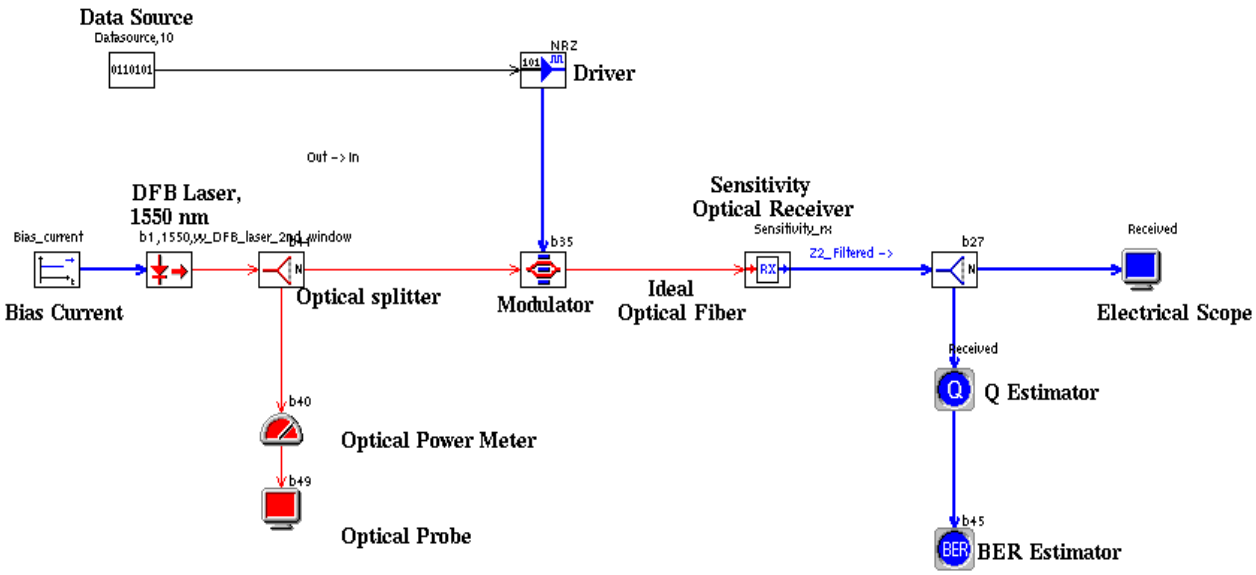

Fig 4.1 (a) Simulation Setup for optimization of bias current

Fig 4.1 (a) shows setup for optimization of bias current. Fig 4.1(b) shows the setup for optimization of amplitude, phase modulators formats combined with RZ and NRZ coding formats.Alcatel Teralight single mode fiber was used as transmission medium whose length is varied from 10km to 100km. It has loss 0.205 dB/ km and dispersion of 8 ps/nm/km.

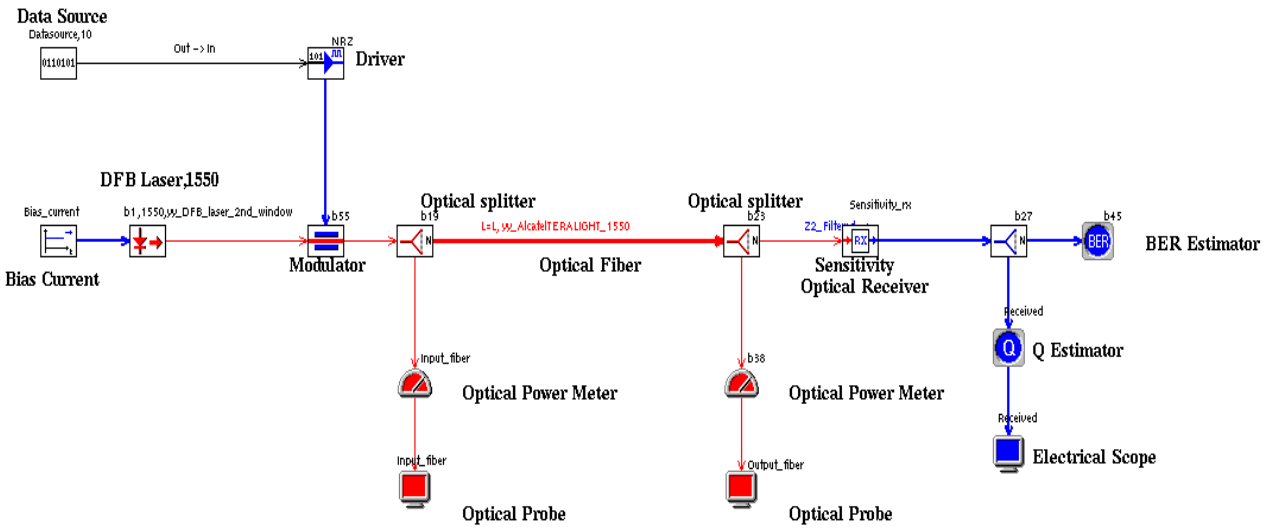

Fig 4.1 (b) Simulation Setup for Optimization of Modulation formats

After modulation signal is transmitted through the fiber. Received optical power can be measured with the help of optical power meter. Signal is detected by the sensitivity receiver and it is analysed with the help of electrical scope, Q estimator and BER estimator in terms of Q factor, BER and eye diagram.

4.4 Result and Discussions

Bias current is varied from 1 mA to 90 mA and output power is ploted against it as shown in figure 4.2. It is observed that below threshold current there is very low output power. Near threshold current there is significant increase in power. Power increase significantly upto 40 mA. And after that output power get saturated.

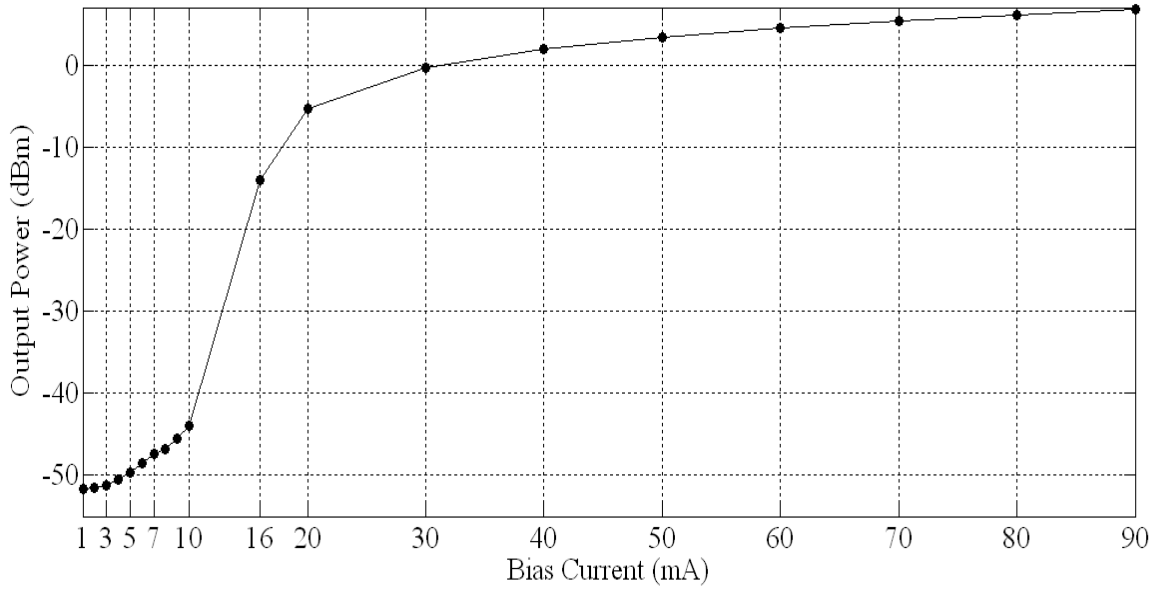

Fig 4.2 Bias current Vs Output Power

After detection of the signal by receiver it is analysed with the help of eye diagram in terms of eye diagram. BER is plotted against bias current as shown in figure 4.3. Here it is observed at bias current value below threshold bit error rate is very high. As bias current is increased above threshold there is significant decrease in bit error rate. At bias current 40 mA bit error reduce to 10^{-40}. If bias current is increased above this value bit error rate remain 10^{-40} up to 70 mA. Further increasing the bias current above 70mA there is increase in bit error rate.

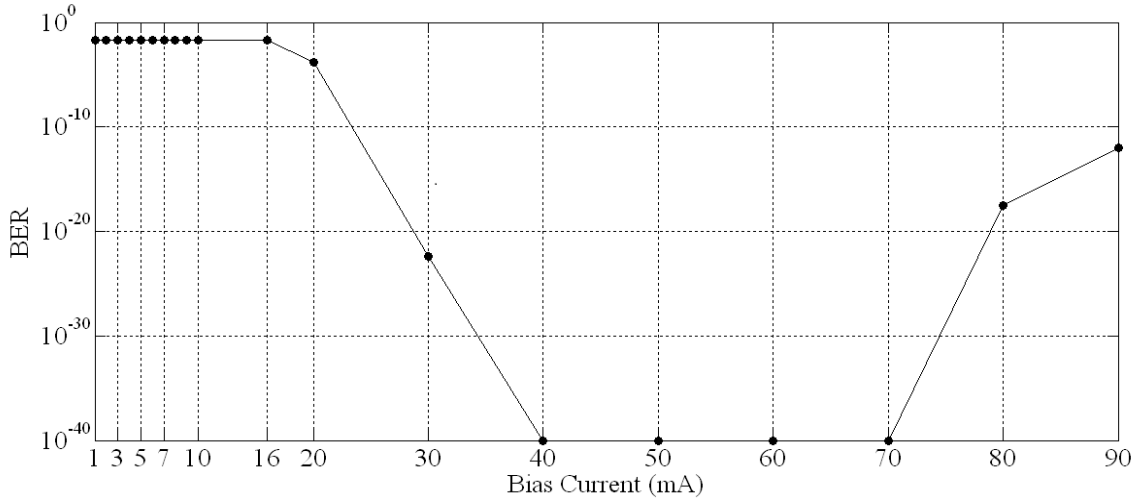

Fig 4.3 Bias Current Vs Bit Error Rate

Q factor variations with bias current are plotted in figure 4.4. It is observed that above threshold current there is sharp increase in Q factor up to 40mA. Above 40mA and up to 60mA there is not much increase in Q factor of signal.

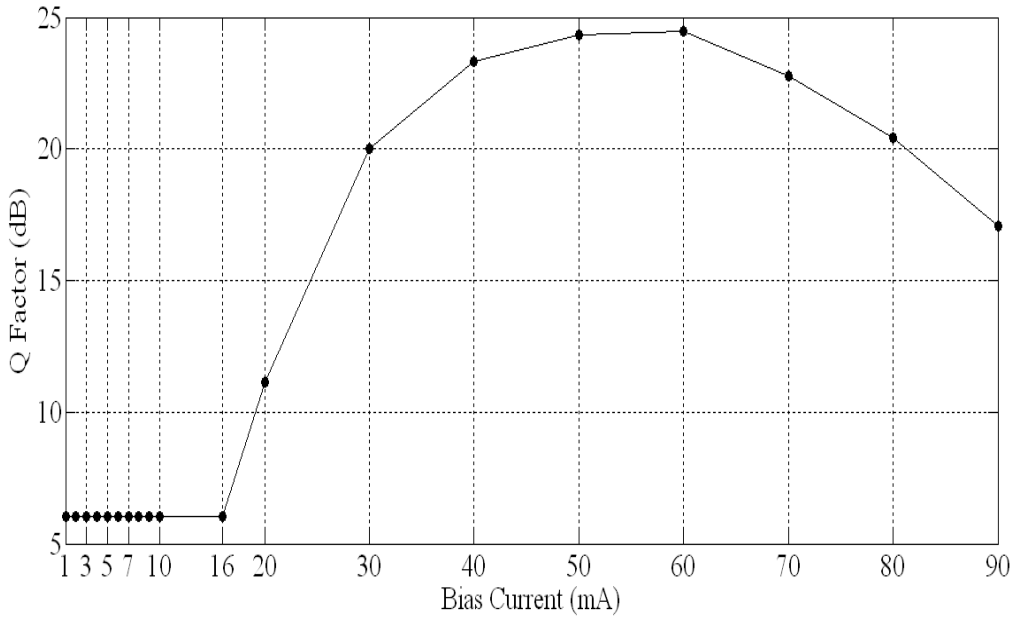

Fig 4.4 Bias Current Vs Q Factor

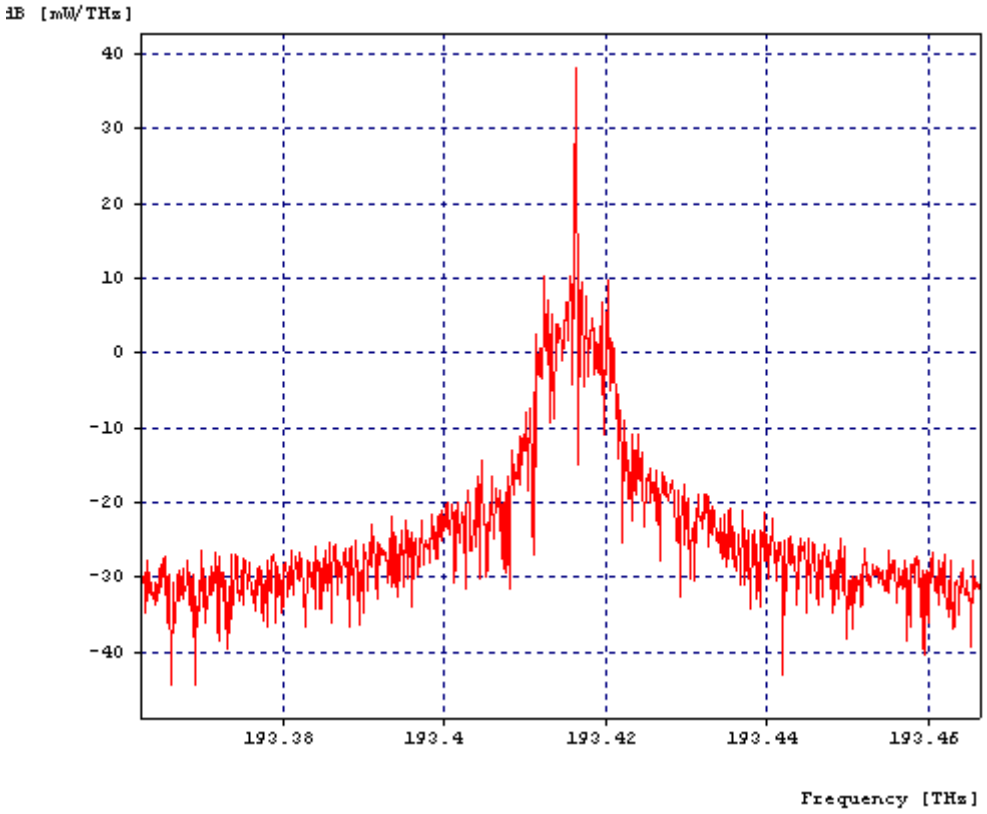

Fig 4.5 Optical Spectrum at I_{bias}=30 mA

The optical spectrum of output signal with a bias current of 30 mA is shown in figure 4.5. This figure shows that the output power has side lobes at central frequency.

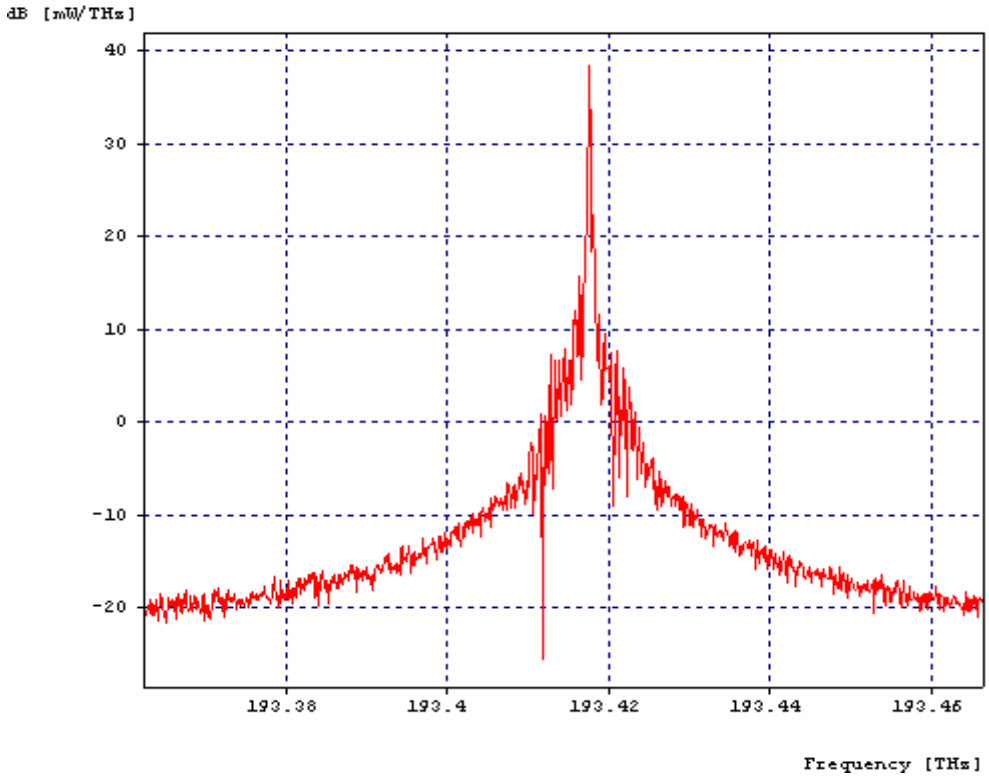

Fig 4.6 Optical Spectrum at I_{bias}=40 mA

The optical spectrum of output signal with a bias current of 40 mA is shown in figure 4.6. This figure shows that there are minimum side lobes at central frequency.

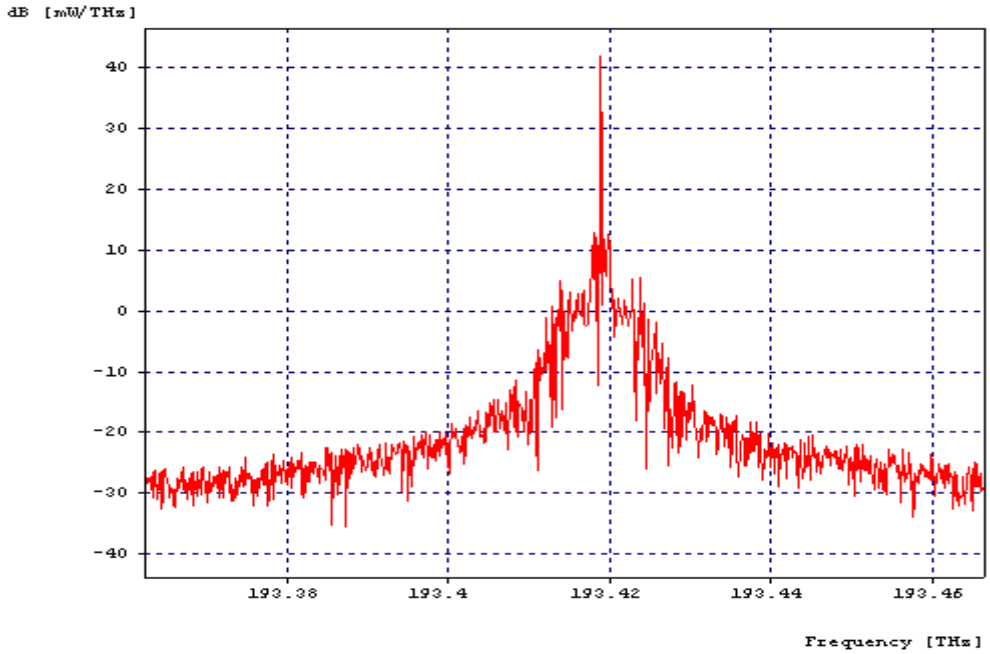

Fig 4.7 Optical Spectrum at I_{bias}=50 mA

The optical spectrum of output signal with a bias current of 50 mA is shown in figure 4.7. This figure shows that the side lobes are again increases at central frequency. So, at 40 mA bias current gives the acceptable output power level.

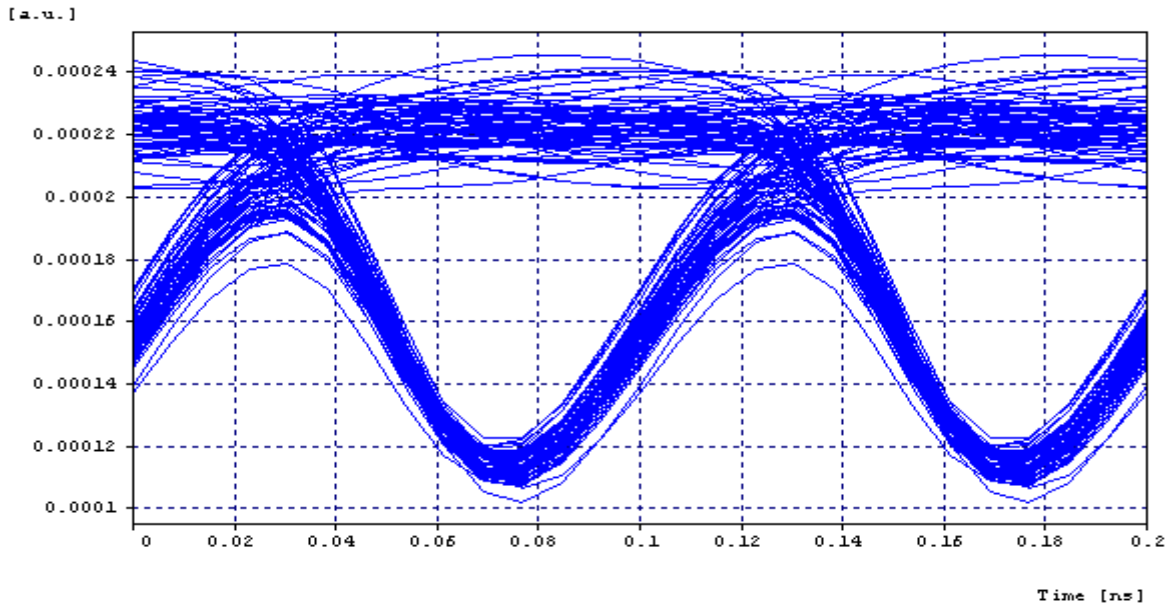

Fig 4.8 Eye Diagram at $I_{bias=}$30 mA

The optical eye diagram of output signal with a bias current of 30 mA is shown in figure 4.8. This figure shows that the eye opening is not acceptable with a bit error rate of 10^{-20}.

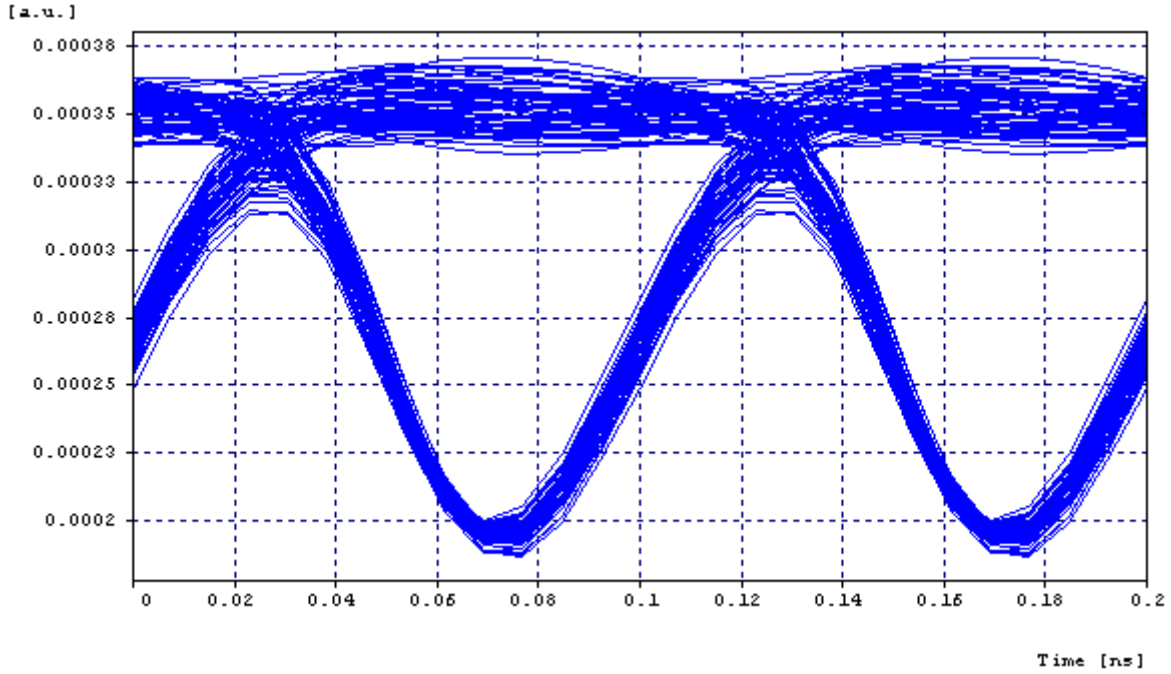

Fig 4.9 Eye Diagram at $I_{bias=}$40 mA

The optical eye diagram of output signal with a bias current of 40 mA is shown in figure 4.9. This figure shows that the eye opening is acceptable with a bit error rate of 10^{-40}.

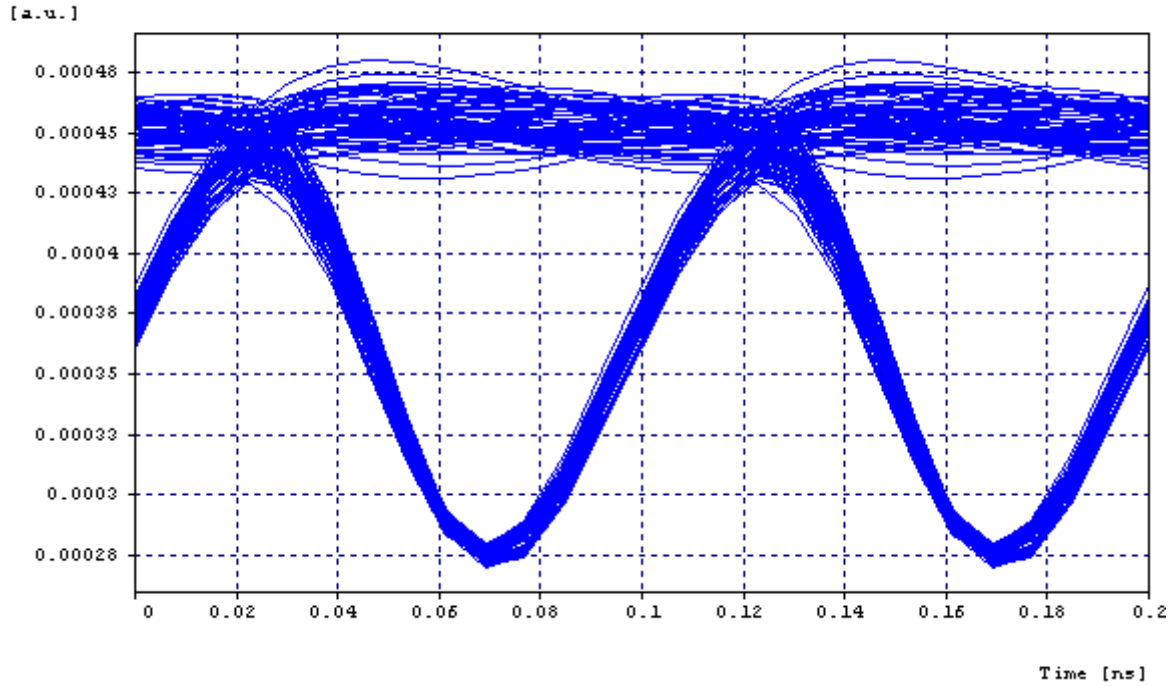

Fig 4.10 Eye Diagram at I_{bias} =50 mA

The optical eye diagram of output signal with a bias current of 50 mA is shown in figure 4.10. This figure shows that the eye opening is also acceptable with a bit error rate of 10^{-40}. Figure 4.11 shows variations of BER with distance as function of distance for RZ and NRZ formats using amplitude modulation. It is observed that NRZ raised cosine give acceptable BER up to maximum distance of 70km.

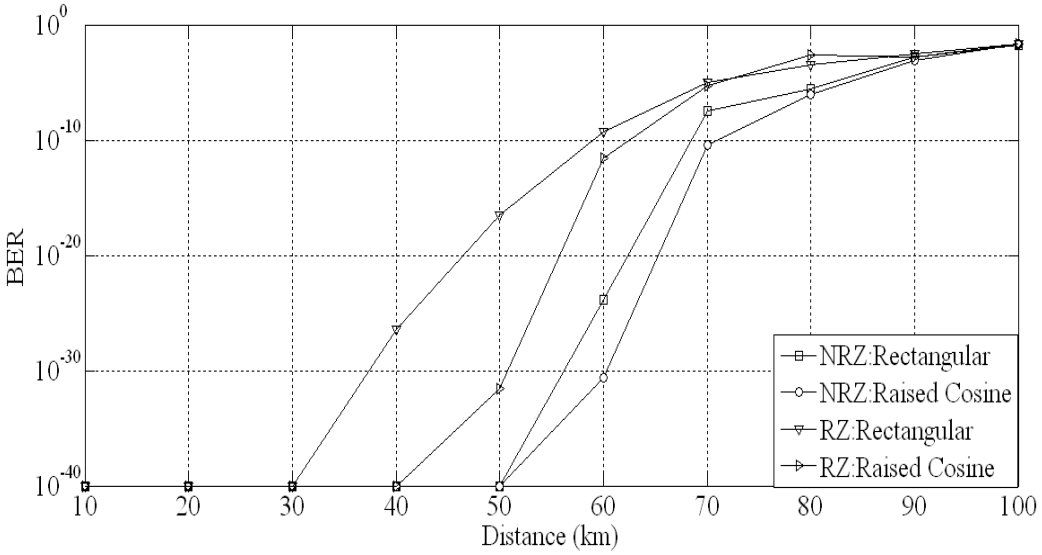

Fig 4.11 Distance Vs BER using Amplitude Modulation at I_{bias}=40 mA

Figure 4.12 shows variations of BER with distance as function of distance for RZ and NRZ formats using phase modulation. It is observed that NRZ rectangular gives acceptable BER up to maximum distance of 90km.

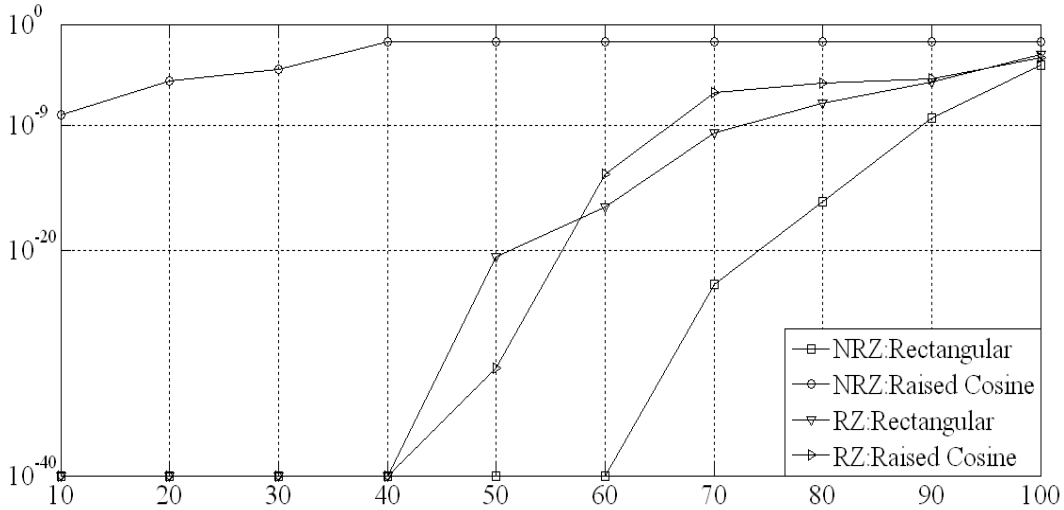

Fig 4.12 Distance Vs BER using Phase Modulation at I_{bias}=40 mA

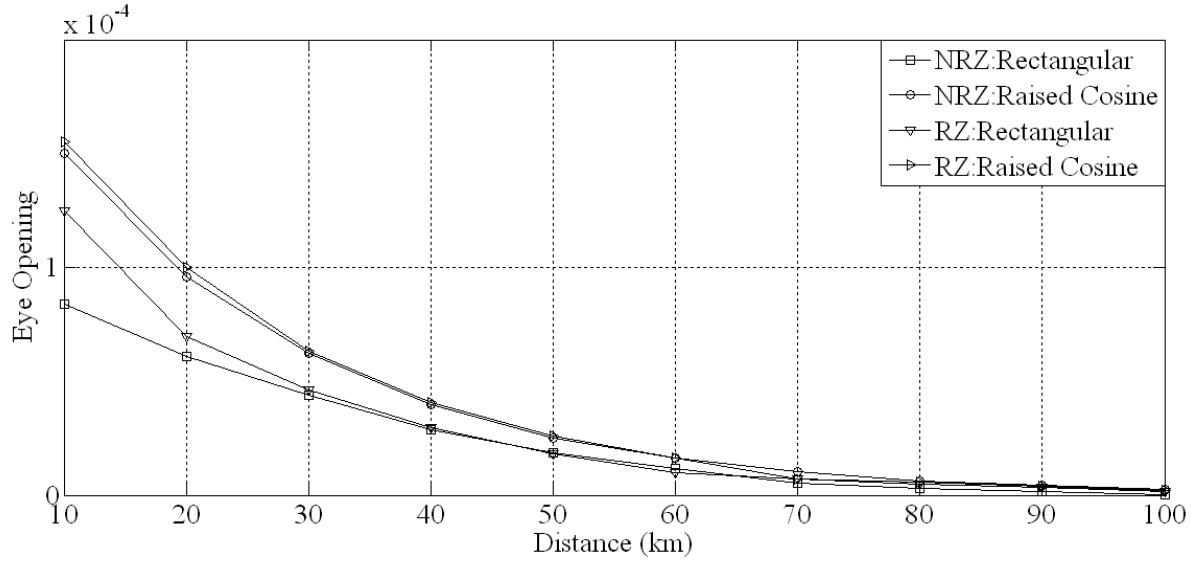

Fig 4.13 Distance Vs Eye Opening using Amplitude Modulation

Figure 4.13 shows variations of eye opening with distance for RZ and NRZ formats using amplitude modulation. It is observed that NRZ raise cosine gives better eye opening up to maximum distance of 70km.

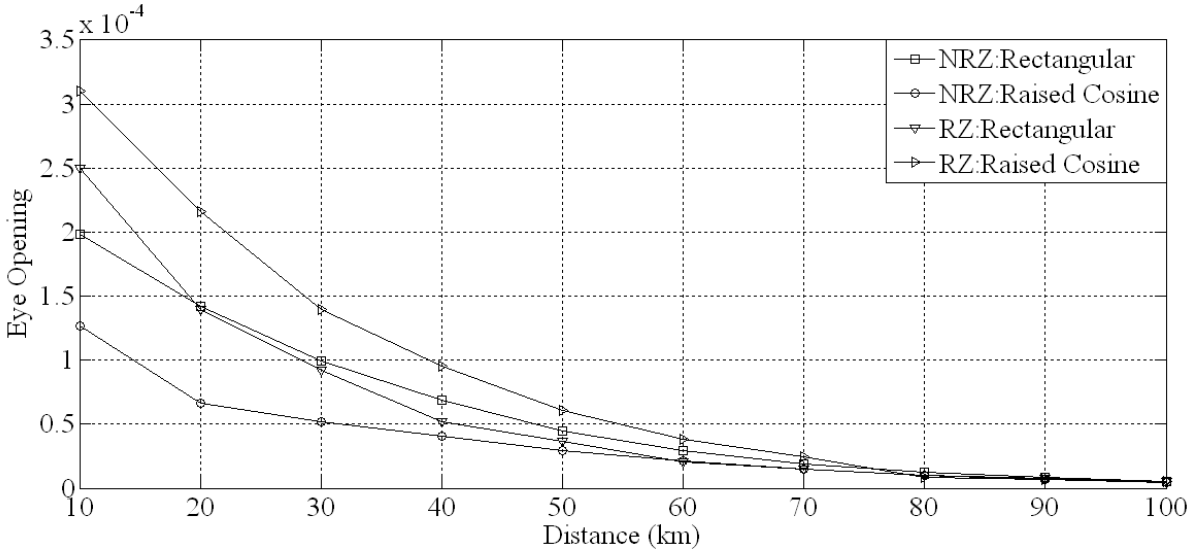

Fig 4.14 Distance Vs Eye opening using Phase modulation

Figure 4.14 shows variations of eye opening with distance for RZ and NRZ formats using phase modulation. It is observed that NRZ rectangular gives better eye opening up to maximum distance of 90km.

4.5 Conclusion

It is concluded that when bias current is increased around threshold current, output power of DFB laser increase sharply. As current is further increased, its output power goes on increasing but after certain value 70 mA it gets saturated. As far as effect of driving current on BER is concerned it decreases sharply as bias current is increased around threshold current. On further increasing the bias current it remain minimum 10^{-40} and after 70 mA it again starts increasing. It is observed that DFB laser with threshold current 15.37 mA when biased at 40mA gives best output optical spectrum with minimum BER when it is modulated by an amplitude modulator. This value of driving current is used to analyse the performance of RZ and NRZ coding formats simultaneous with amplitude and phase modulator and is observed that NRZ raised cosine signal when modulated with amplitude modulator can travel 70 km with acceptable BER 10^{-9}. While NRZ rectangular signal can travel 90 km with acceptable BER 10^{-9}.

Chapter 5 Conclusion and Future Work

The work presented here is emphasized on the performance evaluation of VCSEL and DFB lasers with the optimization of various parameters.

5.1 Conclusion

The impacts produced by the change in ambient temperature and propagation through single mode and multimode fiber for VCSEL are analyzed through eye diagrams and output power evaluation. The plots depict the values of eye opening, BER and output power for different values of temperature and length of single mode and multimode fiber. Through the output power evaluation the output signal is observed at different values of ambient temperature. It is observed that as the temperature increases the output optical power decreases. It can be compensated by increasing the drive current but it limits the life time of the laser due to large current density. It is also observed that if threshold voltage is decreased keeping the temperature constant output power increase. This effect of threshold voltage can be used for compensation of power decreased due to increase in temperature. It can be easily observed multimode fiber can transmit signal with data rate 2 Gb/s with acceptable BER of 10^{-9} up to small distance only. On the other hand, single mode fibers can transmit with same BER to larger distance. With same input power MM fiber can transmit signal with BER 10^{-9} up to distance of 125 meters. Whereas, SM fibers can transmit the signal with same BER up to 3.7 km.

It is concluded from light current characteristics that when bias current is increased around threshold current, then output power of DFB laser increase sharply. As current is further increased, its output power goes on increasing but after certain value 70 mA it get saturated. BER decreases up to 40 mA and remain at its minimum value till bias current is 70 mA, after which it again starts increasing. A laser with threshold current 15.69 mA is drived at 40mA. It gives best output optical spectrum with minimum BER when it is modulated by an amplitude modulator. This value of driving current is used to analyse the performance of RZ and NRZ coding formats simultaneous with amplitude and phase modulator and it is obtained that NRZ raised cosine signal when modulated with amplitude modulator can travel 70km with acceptable BER 10^{-9}. While NRZ rectangular signal can travel 90km with acceptable

BER 10^{-9}. So NRZ rectangular coding format combined with phase modulator can travel long distance with acceptable BER.

5.2 Future Work

In this work, the limitation of VCSEL working at high temperature is discussed. As there are different parameters by which this effect can be compensated. Future work can be extended by using these parameters. Here VCSEL is used with direct modulation; this work can be extended by using VCSEL with external modulator. Modulation plays important roles in any communication system; various advanced modulation coding formats are available. By using DFB laser work can be extended by employing these modulation coding formats with higher data rates.

References

[1] M Arumugam, “Optical fiber communication : An overview”, Pramana Journal of Physics, Vol. 57, pp. 849–869, 2001.

[2] Melanie Ott, “Capabilites and Reliability of LEDs and Laser Diodes” Technology Validation Assurance Group 1997.

[3] G. Keiser, “Optical Fiber Communications”, Tata Mcgraw Hill Publishing Company, Fourth Edition, pp. 40-186.

[4] G.P. Agrawal, “Fiber-Optic Communication Systems”, John Wiley & Sons Publication, Third Edition, pp 77-105, 1997.

[5] J. Tatum and J. Guenter, “Modulating VCSELs”, Honeywell Optoelectonics Application Note,1998.

[6] Harushisa Soda, Ken-ichi Iga, Chiyuki Kitahara and Yasuharu Suematsu, “GaInAsP/InP Surface Emitting Injection Lasers”, Japanese Journal of Applied Physics, Vol. 18, No. 12, pp. 2329-2330, 1979.

[7] N.M. Margalit, S.Z. Zhang and J.E. Bowers “Vertical Cavity Lasers for Telecom Applications”, IEEE Communications Magazine, Vol. 12, No. 31, pp. 164-170, 1997.

[8] C.W. Wilmsen, H. Temkin and L.A. Coldren, “Vertical Cavity Surface Emitting Lasers Design, Fabrication, Characterization and Applications”, Cambridge University Press, pp. 113-159, 1999.

[9] Kenichi Iga, “Surface-Emitting Laser Its Birth and Generation of New Optoelectronics Field”, IEEE Journal on Selected Topics in Quantum Electronics, Vol. 6, No. 6, pp. 1201-1215, 2000.

[10] Joachim Piprek, Dubravko I. Babic, John E. Bowers, “Simulation and analysis of 1.55 μm double-fused vertical-cavity lasers”, Journal of Applied Physics, Vol. 81, No. 8, pp 3386-3386, 1997,

[11] Near M. Margalit, “High-Temperature Long-Wavelength Vertical-Cavity Lasers”, ECE Techincal Report, University of California, pp. 160-160, 1998.

[12] D.N. Payne and W.A. Gambling, “Zero material dispersion in optical fibers,” Electronics Letter, vol. 11, pp. 176–178, 1975.

[13] T. Miya, Y. Terunuma, T. Hosaka, and T. Miyashita, “Ultimate low-loss single-mode fiber at 1.55 μm”, Electronics Letter, vol. 15, pp. 106–108, 1979.

[14] K. Utaka, S. Akiba, K. Sasaki, and Y. Matsushima, “Room-temperature CW operation of distributed-feedback buried-heterostructure InGaAsP/InP lasers emitting at 1570 nm”, Electronics Letter, vol. 17, pp. 961–963, 1981.

[15] S. Kakimoto, A. Takemoto, Y. Sakakibara, Y. Nakajima, M. Fujiwara, H. Namizaki, H. Higuchi, and Y. Yamamoto, “Wavelength dependence of 1.2–1.55 μm InGaAsP/InP p-substrate buried crescent laser diodes”, IEEE Journal of Quantum Electron., vol. 24, pp. 29–35, 1988.

[16] M.C. Amann et al., “Tunable twin-guide laser: a novel laser diode with improved tuning performance”, Applied Physics Letter, vol 54, pp. 2532-2532, 1989.

[17] Biswanath Mukherjee , “Optical WDM Networks”, Springer, pp. 2-6, 2006.

[18] OptSim Technical Staff, “Time Domain Spilt-Step Fiber Simulation Approach,” White Paper of Artis Software Corporation, 1999.

[19] H. Sunnerud, M. Karlsson, and P. A. Andrekson, “A comparison between NRZ and RZ data formats with respect to PMD-induced system degradations”, IEEE Photonics Technology Letters, Vol.13, No. 5, pp. 448–450, 2001.

[20] M.I.Hayee and A.E.Willner, “NRZ versus RZ in 10-40-Gb/s dispersion-managed WDM transmission systems,”IEEE Photonics Technology Letters, Vol. 11, N0. 8, pp. 991-993, 1999.

[21] N. Nishiyama, C. Caneau, M. H. Hu, X. S. Liu, M.-J. Li, R. Bhat, and C. E. Zah, “Long-Wavelength Vertical-Cavity Surface-Emitting Lasers on InP With Lattice Matched AlGaInAs–InP DBR Grown by MOCVD”, IEEE Journal on Quantum Electronics, Vol. 11, NO. 5, pp. 990-998, 2005.

[22] Adil Karim, Joachim Piprek, Patrick Abraham, Dan Lofgreen, Yi-Jen Chiuand, John E. Bowers, “1.55μm Vertical-Cavity Laser Arrays for Wavelength-Division Multiplexing”, IEEE Journal on Quantum Electronics, Vol. 7, NO. 2, pp. 178-183, 2001.

[23] Mikihiro Kajita, Takeshi Kawakami, Masaaki Nido, Akitaka Kimura, Takashi Yoshikawa, Kaori Kurihara, Yoshimasa Sugimoto and Kenichi Kasahara, “Temperature Characteristics of a Vertical-Cavity Surface-Emitting Laser with a Broad-Gain Bandwidth”, IEEE Journal on Quantum Electronics, Vol. 1, NO. 2, pp. 654-660, 1995

[24] P. V. Mena J. J. Morikuni S.M. Kang, A. V. Harton and K. W. Wyatt, “A Simple Rate-e quation-Based Thermal VCSEL Model”, Journal Of Lightwave Technology, Vol. 17, No. 5, pp. 865-872, 1999.

[25] Keun Ho Rhew, Su Chang Jeon, Dae Hee Lee , Byueng-Su Yoo , Ilgu Yun, “Reliability assessment of 1.55-lm vertical cavity surface emitting lasers with tunnel junction using high-

temperature aging tests", Journal on Microelectronics Reliability, vol. 49, pp. 42–50, 2009
[26] Robert **A.** Morgan, "VCSEL research, development and applications at Honeywell," Honeywell Technology Center.
[27] N. Laurand, S. Calvez, H.D. Sun, M.D. Dawson, J.A. Gupta and G.C. Aers, "C-band emission from GaInNAsSb VCSEL on GaAs", Electronics Letters, Vol. 42, No. 1, pp. 1-2 2006.
[28] Feng-Ming Lee, Chia-Lung Tsai, Chih-Wei Hu, Kun-Fu Huang, Meng-Chyi Wu, and Sun-Chien Ko, "1.3-μm GaInAsN Vertical Cavity Surface-Emitting Lasers by Oxide-Planarized and Surface-Relief Processes for Single-Mode Operation", IEEE Electron Device Letters, Vol. 28, NO. 2, pp. 120-122, 2007.
[29] Yoshitsugu Wakazono, Katsuya Kikuchi, Atsushi suzuki, Kenji suzuki, Shuji suzuki, Takayuki yamaguchi, Hiroshi nakagawa, Masahiro aoyagi and Osamu ibaragi, "Fundamental Analysis of VCSEL Emission for Evaluation of Optical Coupling Efficiency", Electronics Packaging Technology Conference,Vol. 5, pp. 380-383, 2005.

[30] S. F. Yu, "Dynamic Behaviour of Vertical-Cavity Surface-Emitting Lasers", IEEE Journal Of Quantum Electronics, Vol. 32, No. 7, pp. 1168-1179, JULY 1996.
[31] A. Mohd Sharizal, Paul O. Leisher, Kent D. Choquette et al. "Effect of oxide aperture on the performance of 850 nm vertical-cavity surface-emitting lasers", Optik Journal, vol. 120, pp. 121–126, 2009.
[32] A.A. Dyomina, V.V. Lysak et al., "Temperature behaviour of top mirror reflection spectrum in intra-cavity-contacted oxide-confined vertical-cavity surface-emitting lasers", Optics and Lasers in Engineering, Vol. 46, pp. 211–216, 2008.

[33] Michel Krakowski, Daniel Rondi, "Ultra-Low-Threshold, High-Bandwidth, Very-Low-Noise Operation of 1.52 μm GaInAsP/InP DFB Buried Ridge Structure Laser Diodes Entirely Grown by MOCVD," IEEE Journal Of Quantum Electronics. Vol 25, No. 6, pp. 1346-1352, 1989.
[34] G.F.Barlow and K.A.Shore, "Threshold gain and threshold current analysis of circular grating DFB organic semiconductor lasers," IEE Proc.-Optoelectron., Vol. 148, No. 4, pp. 165-170, 2001.

[35] Manoj Kumar, Ajay K. Sharma, T.S.Kamal, Jagjit Singh Malhotra, "Comparative investigation and suitability of various data formats for 10 Gb/s optical soliton transmission links at different chirps", Optik, vol 120, pp. 330-336, 2009.

[36] Aihan Yin, Li Li Xinliang Zhang, "Analysis of modulation format in the 40 Gbit/s optical communication system", Opt. Int. J. Light Electron. Opt., pp. 1-8, 2009 .

[37] K. Kasahara, "VSTEP-based smart pixels," IEEE J. Quantum Electron**.,** Vol. 29, pp. 757-768, 1993.

[38] M. G. Peters, F. H. Peters, D. B. Young, J. W. Scott, B. J. Thibeault, and L. A. Coldren, "High wallplug efficiency vertical-cavity surface emitting quantum-well lasers and its application for estimation of high-speed modulation limit," IEEE Journal on Quantum Electronics, vol. 29, pp. 885-895, 1993.

[39] M. Kajita, T. Numai, K. Kurihara, T. Yoshikawa, H. Saito, Y. Sugimoto, M. Sugimoto, H. Kosaka, I. Ogura, and K. Kasahara, " Thermal analysis of laser-emission surface-normal optical devices with a vertical cavity." Jpn. Journal on Applied Physics, vol. 33, pp. 859-863, 1994.

[40] D. B. Young, J. W. Scott, F. H. Peters, M. G. Peters, M. L. Majewski, B. J. Thibeault, Scott W. Corzine, and L. A. Coldren, "Enhanced performance of offset-gain high-barrier vertical-cavity surface-emitting lasers," IEEE Journal on Quantum electronics, vol. 29, pp. 2013-2022, 1993.

[41] S**.** A. Chalmers, K. L. Lear, and K. P. Killeen, "Low resistance wavelength-reproducible p-type (A1,GaAs) distributed Bragg reflectors grown by molecular beam epitaxy," Appl. Phys. Lett., vol. 62, pp. 1585-1587, 1993.

[42] Tatsuya Takeshita, Toshiaki Kagawa, "Degradation Behavior of 850-nm Vertical-Cavity Surface-Emitting Lasers With an Air-Post Index-Guide Structure," Journal Of Lightwave Technology, Vol. 20, NO. 4, pp. 722-728, 2002.

[43] Yuan Xue-guang , Zhang Jin-nan, Zhang Yang-an, Zhang Ming-lun, Huang Yongqing, Ren Xiao-min, "Experimental demonstration and analysis of all-optical label swapping based on RZ-DQPSK/IRZ-ASK modulation format", The Journal of China Universities of Posts and Telecommunications, Vol. 17, No. 1, pp 101–105, 2010.

[44] Mohammad F. Alam, Mohammad A. Karim and Saiful Islam, "Effects of Structural Parameters on the External Optical Feedback Sensitivity in DFB Semiconductor Lasers", IEEE Journal Of Quantum Electronics, Vol. 33, No. 3, pp. 424-433,1997.

[45] R. Steingruber, M. Mohrle, "Design aspects for the fabrication of gratings for DFB-lasers by direct write electron-beam lithography", Microelectronic Engineering Vol. 78, No. 79, pp. 51-54, 2005.

[46] Ezra Ip and Joseph M. Kahn, "Power Spectra of Return-to-Zero Optical Signals", Journal Of Light wave Technology, Vol. 24, No. 3, pp. 1610-1618, 2006.

[47] James E.A. Whiteaway, G.H.B. Thompson, Andrew J. Collar and Christopher J. Armistead, "The Design and Assessment of λ/4 Phase-Shifted DFB Laser Structures", IEEE Journal Of Quantum Electronics, Vol. 25, No. 6, pp. 1261-1279, 1989.

[48] Jose A.P. Morgado, Carlos A.F. Fernandes, Jose B.M. Boavida, "Novel DFB laser structure suitable for stable single longitudinal mode operation", A Journal OF Optics & Laser Technology, Vol. 42, pp. 975–984, 2010.